

AD-A214 714

ACTION PAGE

Form Approved
OMB No. 0704-0188

On average 1 hour per research, including the time for reviewing instructions, searching existing data sources, gathering the collection of information. Send comments regarding this burden estimate or any other aspect of this form, to Washington Headquarters Services, Directorate for Information Operations and Reports, 1215 Jefferson Avenue, Washington, DC 20540.

1. AGENCY USE ONLY (Leave blank)		2. REPORT DATE April 12, 1984	3. REPORT TYPE AND DATES COVERED Final (9/30/83-3/31/84)	
4. TITLE AND SUBTITLE NEW METALLOPHILIC COLLOIDAL CERAMICS			5. FUNDING NUMBERS 65502F 3005/A1	
6. AUTHOR(S) G.B.. Alexandeer and J.K. Weeks Jr				
7. PERFORMING ORGANIZATION NAME(S) AND ADDRESS(ES) Technical Research Associates 410 Chipeta Way, Suite 222 Salt Lake City, Utah 84108			8. PERFORMING ORGANIZATION REPORT NUMBER 1644 AFOSR TR 89 - 1644	
9. SPONSORING / MONITORING AGENCY NAME(S) AND ADDRESS(ES) AFOSR BLDG 410 BAFB DC 20332-6448			10. SPONSORING / MONITORING AGENCY REPORT NUMBER F49620-83-C-0162	
11. SUPPLEMENTARY NOTES				
12a. DISTRIBUTION / AVAILABILITY STATEMENT dissemi			12b. DISTRIBUTION CODE	
13. ABSTRACT (Maximum 200 words) <div style="text-align: right; font-size: 2em; font-weight: bold;">DTIC ELECTE NOV 29 1989 S B D</div>				
14. SUBJECT TERMS			15. NUMBER OF PAGES 76	
			16. PRICE CODE	
17. SECURITY CLASSIFICATION OF REPORT unclassified	18. SECURITY CLASSIFICATION OF THIS PAGE unclassified	19. SECURITY CLASSIFICATION OF ABSTRACT	20. LIMITATION OF ABSTRACT	

NSN 7540-01-280-5500

Standard Form 298 (890104 Draft)
Prescribed by ANSI Std. Z39-18
298-01

89 11 037

1644

~~XXXXXXXXXX~~

FINAL REPORT
NEW METALLOPHILIC COLLOIDAL CERAMICS
DR. GUY B. ALEXANDER

F49620-83-C-0162

TECHNICAL RESEARCH ASSOCIATES
410 Chipeta Way, Suite 222
Salt Lake City, Utah 84108

September 30, 1983 - March 30, 1984

NEW METALLOPHILIC COLLOIDAL CERAMICS

Phase I Report

TABLE OF CONTENTS

	Page
1. Executive Summary.....	3
2. Phase I Objectives and Work Statement.....	4
3. Phase I Conclusions.....	5
4. Phase I Results - Details.....	13
5. Discussion of Results.....	36
6. Commercial Potential.....	61
7. Proposed Publications	64
8. Personnel.....	64
9. Interactions.....	64
10. New Discoveries.....	64
11. M. R. Plichta Report.....	66
12. J. G. Byrne Statement.....	75



Accession For	
NTIS GSA&I	<input checked="checked" type="checkbox"/>
DTIC TAB	<input type="checkbox"/>
Unannounced	<input type="checkbox"/>
Justification	
By	
Distribution/	
Availability Codes	
Dist	Avail and/or Special
A-1	

FIGURES

	Page
1. Inert Atmosphere Box.....	6
2. Coprecipitation Apparatus.....	7
3. Hardness After Anneal.....	12
4. Grain Growth vs. T.....	16
5. Cu(NO ₃) Titration Curve.....	17
6. Cu - Al Phase Diagram.....	22
7. Micrograph: Alumina Sol.....	27
8. Micrograph: Control.....	28
9. Micrograph: Al Cu Mg - Alumina.....	29
10. Micrograph: Al Cu Mg - Alumina.....	30
11. Micrograph from Micron Associates: Control.....	32
12. Micrograph from Micron Associates: ODS with Thoria....	33
13. Micrograph from Micron Associates: ODS with Aluminum..	34
14. Solubility of Silica vs. Particle Size.....	39
15. Solubility of Silica vs. pH.....	40
16. Colloidal Particle Growth.....	41
17. Aggregates of Discrete Particles.....	44
18. Aggregates and Coalescence.....	45
19. Micrograph TD Nickel.....	49
20. TD Nickel Data.....	50
21. TD Nickel Data.....	52
22. IPS vs. % Filler by Volume.....	55
23. IPS vs. Strength - TD Nickel.....	56
24. Reactions of Colloidal Oxides with Metals.....	58
25. ODS Aluminum Flow Sheet.....	59

1. Executive Summary

In this study, TRA has examined the possibility of using alumina and/or thoria for dispersion hardening of aluminum base alloys. Thoria apparently is not wetted by the aluminum alloy, and hence does not appear to be a candidate for the intended use. On the other hand, alumina is wetted and has been dispersed in a submicron state. The opportunity to produce aluminum alloys with superior high temperature strength is real.

The conditions for wetting submicron alumina into a molten alloy of aluminum-copper-magnesium have been demonstrated. This was accomplished by adding copper-alumina master mix slugs to molten aluminum-magnesium. The alloy containing the dispersed oxide was cast and the resulting metal analysed by electron microscopy and hardness after working followed by annealing. Hardness showed retention of properties on annealing. The micrographs showed alumina dispersed uniformly throughout the cast structure at an interparticle (IPS) spacing in the range of 150-200 millimicrons. This is even smaller than the spacing of particles in TD Nickel. Control of IPS at any level from 100 millimicrons and up has been demonstrated.

The new alloy, called oxide dispersion strengthened aluminum or ODS aluminum, is expected to have useful metallurgical strength, at 500-550°C, and thus increase the useful temperature range of aluminum base alloys by at least 200 centigrade degrees.

2. Phase I Objectives and Work Statement

(Copied from the proposal)

2.1 Phase I Objectives.

It is the objective of Phase I of this project to demonstrate the feasibility of modifying the surface of colloidal oxide particles to make them metallophilic. Another objective of Phase I is to use molten aluminum as a model system, and attempt to duplicate the silica-mercury-sodium experiment using aluminum in place of mercury.

2.2 Phase I Work Statement

Task 1. Build an apparatus to test the concept.

Task 2. Study surface modification of ceramic oxides in mercury and molten aluminum and aluminum systems as a function of:

- a) wetting metals
- b) excess oxygen
- c) atmosphere in dry box
- d) oxide type
- e) oxide precoating
- f) various combinations of above variables

Task 3. Propose a theory to explain the observations.

Task 4. Characterize the colloidal ceramic particles from Task 2 using TEM.

Task 5. Characterize the colloidal ceramic-aluminum composite for improvements in hardness after casting, working and annealing.

Task 6. Final Report.

3. Phase I Conclusions

It has been shown that colloidal (about 30 millimicron) alumina particles can be reacted with metallic magnesium in a molten aluminum matrix, and that thereafter said colloidal particles are wetted by molten alloys of aluminum, magnesium and copper. Colloidal thoria particles do not react, are not wetted by the same alloy, are rejected by the alloy during freezing after casting and appear at the grain boundaries. The feasibility of oxide dispersion strengthening (ODS) cast aluminum alloys has been proven.

Nomenclature

In this report, the following nomenclature is used:

ODS Aluminum - Oxide Dispersion Modified Aluminum

OM Copper - Oxide Modified Copper

AM Copper - Alumina Modified Copper

TM Copper - Thoria Modified Copper

Conclusions by Tasks:

Task 1. An apparatus was assembled to test the concept. Figure 1 shows the inert atmosphere box and Figure 2 shows the system used to coprecipitate the copper-metal oxide master batch.

Task 2. Surface modifications of alumina and thoria were studied as a function of a number of variables with the results listed below:

Controlled Atmosphere Glove Box

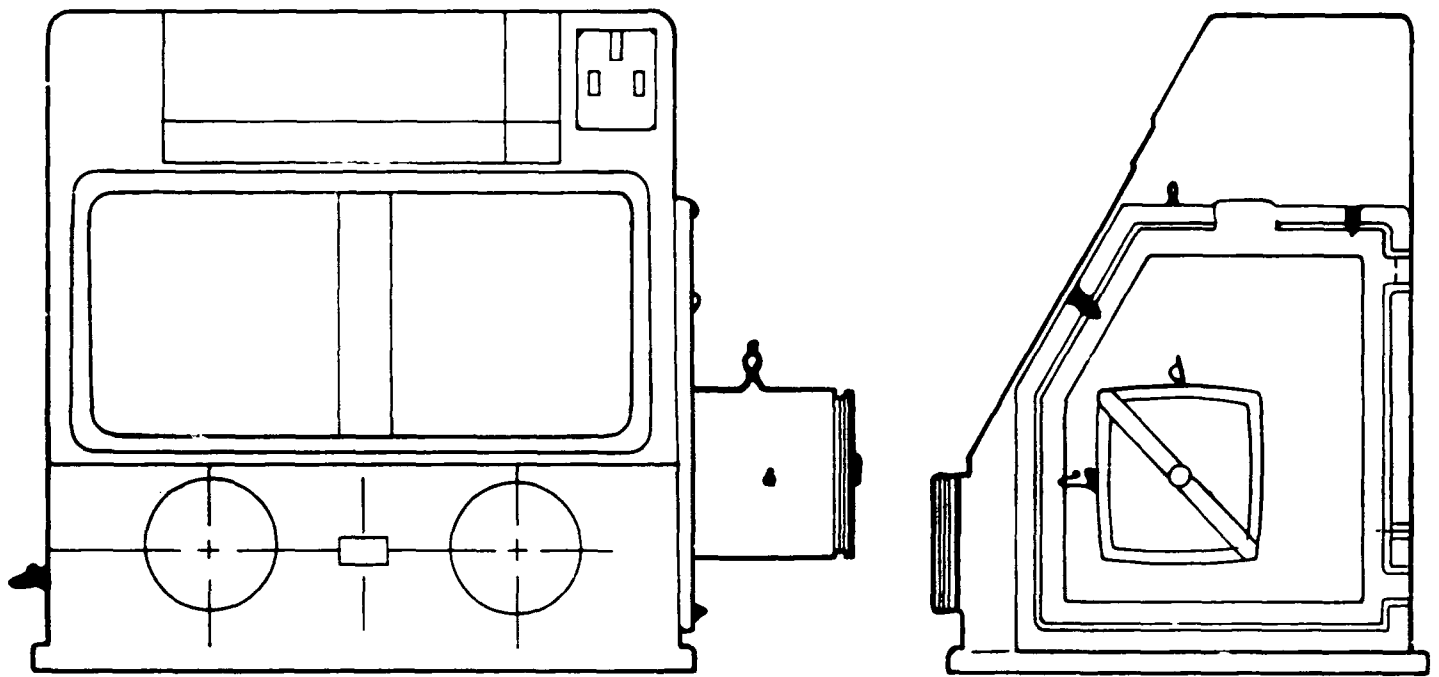


FIGURE 1

Copper - Alumina Coprecipitation Apparatus

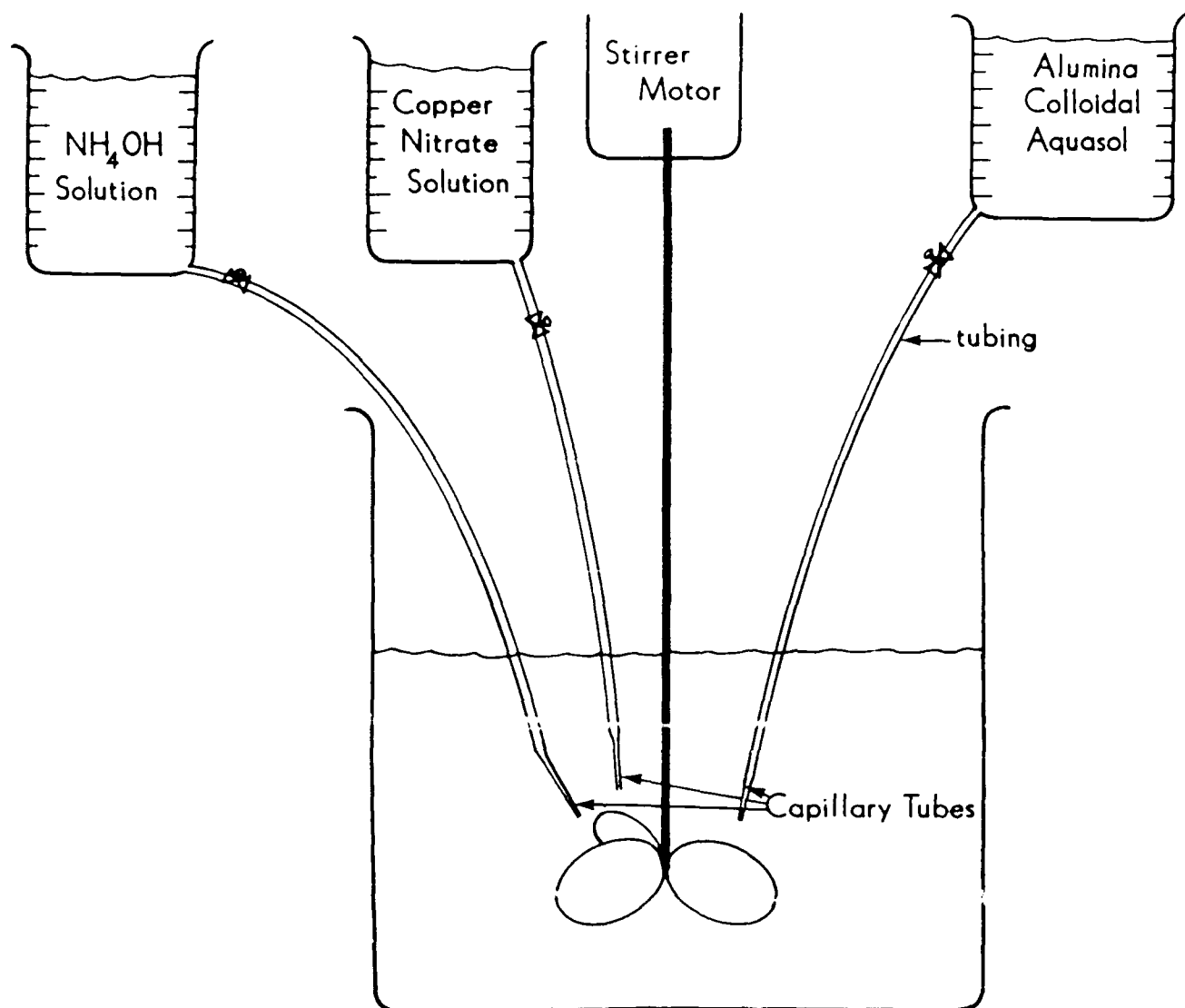


FIGURE 2

Variable	Alumina	Thoria
wetting metals	magnesium causes wetting aluminum will not cause wetting	neither magnesium nor aluminum react and hence do not cause wetting
excess oxygen	Opinion: causes dewetting	
atmosphere	argon allows wetting nitrogen allows wetting oxygen defeats wetting	no wetting with any atmosphere
powder surface area	AM Copper does not dissolve and/or disperse readily in the melt	TM Copper does not dissolve
copper slug	AM Copper slug dissolves slowly. During dissolution, the reaction of magnesium with the alumina wets the latter into the melt.	
combinations	any variable which prevents wetting by itself will also prevent wetting regardless of combination used.	

The combination that promotes wetting is summarized as follows:

AM copper powder is cold pressed, sintered in hydrogen, protected from air (oxygen), and dropped into a molten alloy of aluminum-magnesium. As the copper dissolves in the melt, the alumina reacts with the magnesium and becomes metallophilic. Time must be allowed for the copper and alumina to diffuse throughout the melt, since otherwise chunks of the slugs, infiltrated

by the molten alloy, will persist. These chunks become an aluminum copper intermetallic, having high copper and alumina content, which is reminiscent of the AM copper master batch.

The above points up a problem which must be solved in Phase II, namely: a way to stir or otherwise homogenize the molten alloy must be found.

Task 3. The theory regarding wetting of colloidal oxides in molten aluminum is summarized as follows:

- A metal which thermodynamically reduces the colloidal oxide or reacts therewith will on reaction in the absence of oxygen cause the colloid to become metallophilic. In time, excess magnesium will totally reduce alumina to magnesia and aluminum. When time in the melt is limited, magnesium forms a sub-oxide layer on alumina and causes alumina to be wetted by aluminum. In this project the time required to reduce the alumina is much greater than 1 hour, the maximum melt time. Magnesium and aluminum will not react with thoria and will not promote wetting.

- Conditions of solution, including (a) excess oxygen in the system and b) the form of the AM copper master batch, must be controlled in order to get wetting. Dissolving a solid AM copper (free of copper oxide) slug slowly in the molten aluminum-magnesium allows the wetting reactions to occur as copper dissolves exposing the alumina. On the other hand, when AM copper powder was added to the molten alloy, the powder did not dissolve.

Rather, a glassy looking mass high in alumina and copper formed around the powder. This apparently stopped the reaction. Wetting of the alumina did not occur. The explanation may be that oxygen in the system which had reacted with the AM copper caused a skin of alumina-magnesia to be formed around the powder particles, preventing contact of the colloidal alumina by magnesium, and wetting of the alumina could not occur.

When AM copper powder is cold pressed, sintered in hydrogen, and the slug is maintained in a non-oxidizing atmosphere until it is added to the melt, the copper dissolves slowly, allowing magnesium to react with the alumina and wetting occurs.

Another explanation might be that if powder is used in place of a slug, the molten aluminum has difficulty displacing gas from the powder. Reduction of surface area by making slugs allows this dissolving-wetting barrier to be overcome.

The details and further discussions of wetting are found in the following sections:

4.2.1 Dispersions of OM copper powder in aluminum melts.

4.2.2 Dispersion of OM copper pellets in aluminum melts.

4.2.5 Discussion

5.2 TD Nickel - welding

5.3 ODS Aluminum - wetting

These details give the back up for the conclusions presented above.

Task 4. Electron micrographs of the ODS alloy were prepared by Professor M. R. Plichta, University of Utah and Micron Associates, Wilmington, Delaware.

Conclusions from these studies show that 30 millimicron alumina particles are present in the cast alloy at an interparticle spacing of about 200 millimicrons. Calculation of IPS is about 150 millimicrons. (See section 5.1.3 for a discussion of interparticle spacing.) X-ray diffraction was used to confirm the particle composition.

In the case of TD Nickel, a thoria strengthened nickel formerly produced by DuPont, IPS was about 300-500 millimicrons. Reasoning by analogy, and recognizing that the high temperature yield strength and stress rupture of TD Nickel were equivalent at 1250° C to a control at 870° C, then one might expect that an ODS aluminum alloy would have strength at 500° C equivalent to a control alloy at 300° C. This is in line with the results in Inman with SAP (Iron Age, April 28, 1955, p. 104-106) in which he claims that SAP at 550° C is equivalent in strength to unmodified aluminum at 300° C. SAP is sintered aluminum powder.

Task 5. Characterizing the ODS aluminum alloy for hardness after casting, working and annealing was difficult because of the intermetallics in the system. However, we were able to show that ODS aluminum lost less hardness on annealing than did the unmodified alloy (Figure 3).

In Figure 3, the control lost hardness because of dissolution of the intermetallic precipitates. The ODS alloy lost some hardness as the intermetallic dissolved, but retained hardness due to oxide dispersion hardening.

With regard to high temperature strength, if one reasons

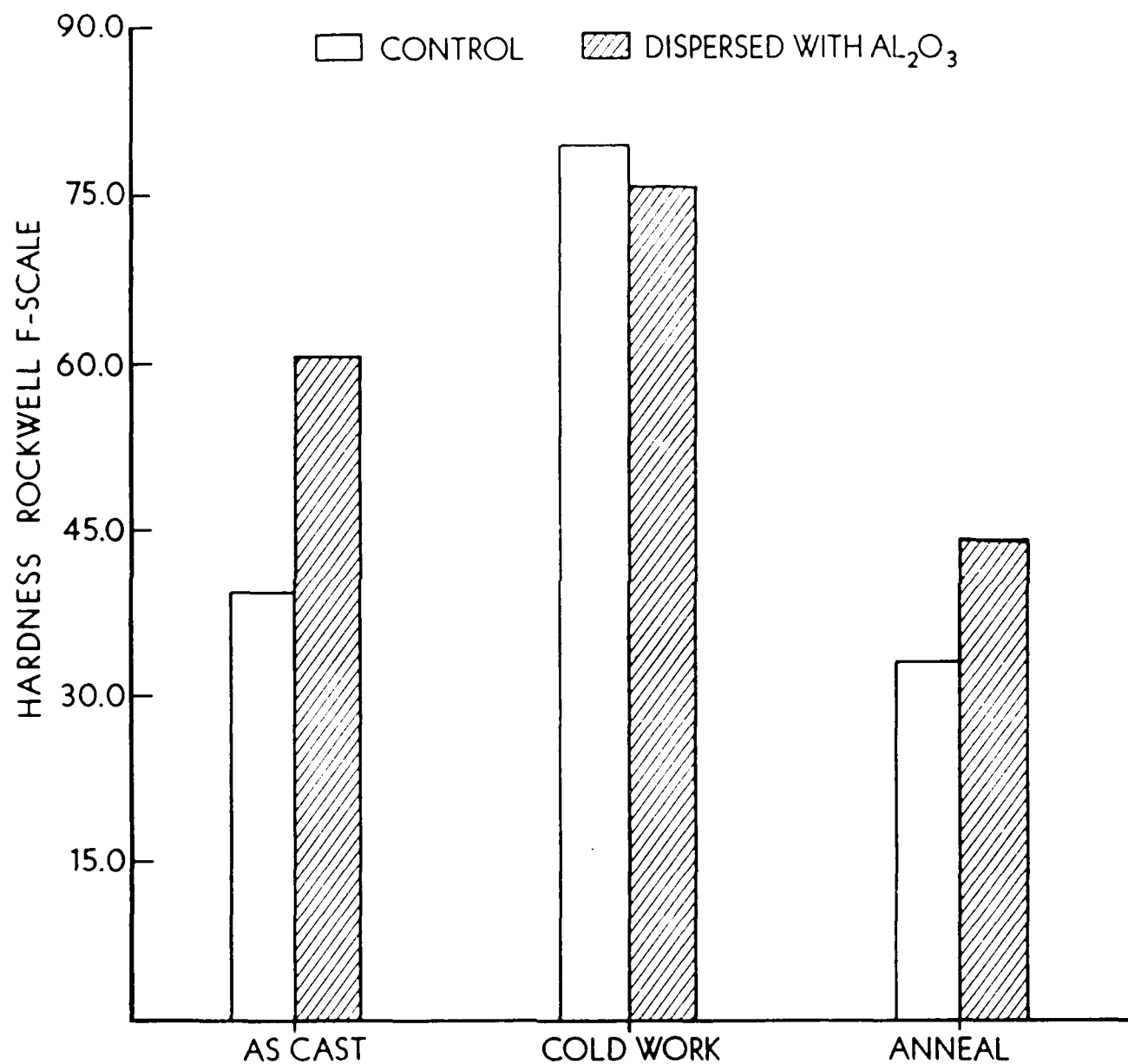


FIGURE 3

by analogy and if one accepts the relationship between ODS Aluminum and TD Nickel, then there seems little doubt about the conclusion reported under Task 4, namely that ODS Aluminum of TRA will have outstanding high temperature strength at 500-550° C and be useful in that temperature range for use in piston engines and the like.

4. Experimental Procedure and Results

4.1 Procedure

4.1.1 Colloidal Oxide Particle Preparation

Colloidal sized oxide particles of thoria and alumina were prepared in the form of an aqueous sol as a starting point in order to produce ODS aluminum.

Alumina is commercially available in submicron particle size ranges. Remet Corporation of Utica NY supplied the alumina powder which was a part of this research. An aqueous sol was prepared by combining 358 grams of water with 2.4 g. of 70% nitric acid in a mixer at room temperature. Forty grams of the alumina powder was added to this mixture over a period of 10 to 15 minutes with vigorous agitation. The sol was then ready for use. Alumina was also prepared by simultaneously adding a solution of aluminum nitrate and ammonium hydroxide to a vigorously agitated solution. This will be discussed further in section 4.1.3.

Colloidal sized thoria particles are not available commercially. Thoria sols were prepared as outlined by Yates (US Patent 3,162,604 to Paul C. Yates, assigned to E. I. duPont

1962). Thoria sols were prepared as follows:

Five hundred grams of thorium nitrate tetrahydrate was dissolved in 810 cc of distilled water and placed in an agitated mixer. To the mixer, a solution of 229 grams of oxalic acid dihydrate dissolved in 2180 cc of distilled water was added dropwise at a rate of 10 cc per minute. The thorium oxalate precipitated out of the solution was filtered and washed with distilled water and dried. The thorium oxalate was then placed into a furnace where it was calcined in air at 650° C for 2 hours, which produced thorium oxide or thoria. The calcined thoria had an average crystallite size of 10 to 20 millimicrons.

Twenty grams of the thoria powder was then added to 80 grams of water and 10 grams of a 10% $\text{Th}(\text{NO}_3)_4$ solution and heated with stirring at 80° C for 12 minutes. The thoria dispersed into the solution and formed a stable sol.

Oxides of calcium, magnesium and zirconium were also ground to less than 100 mesh and were used for initial wetting studies.

4.1.2 OM Copper Background

OM Coprecipitation.

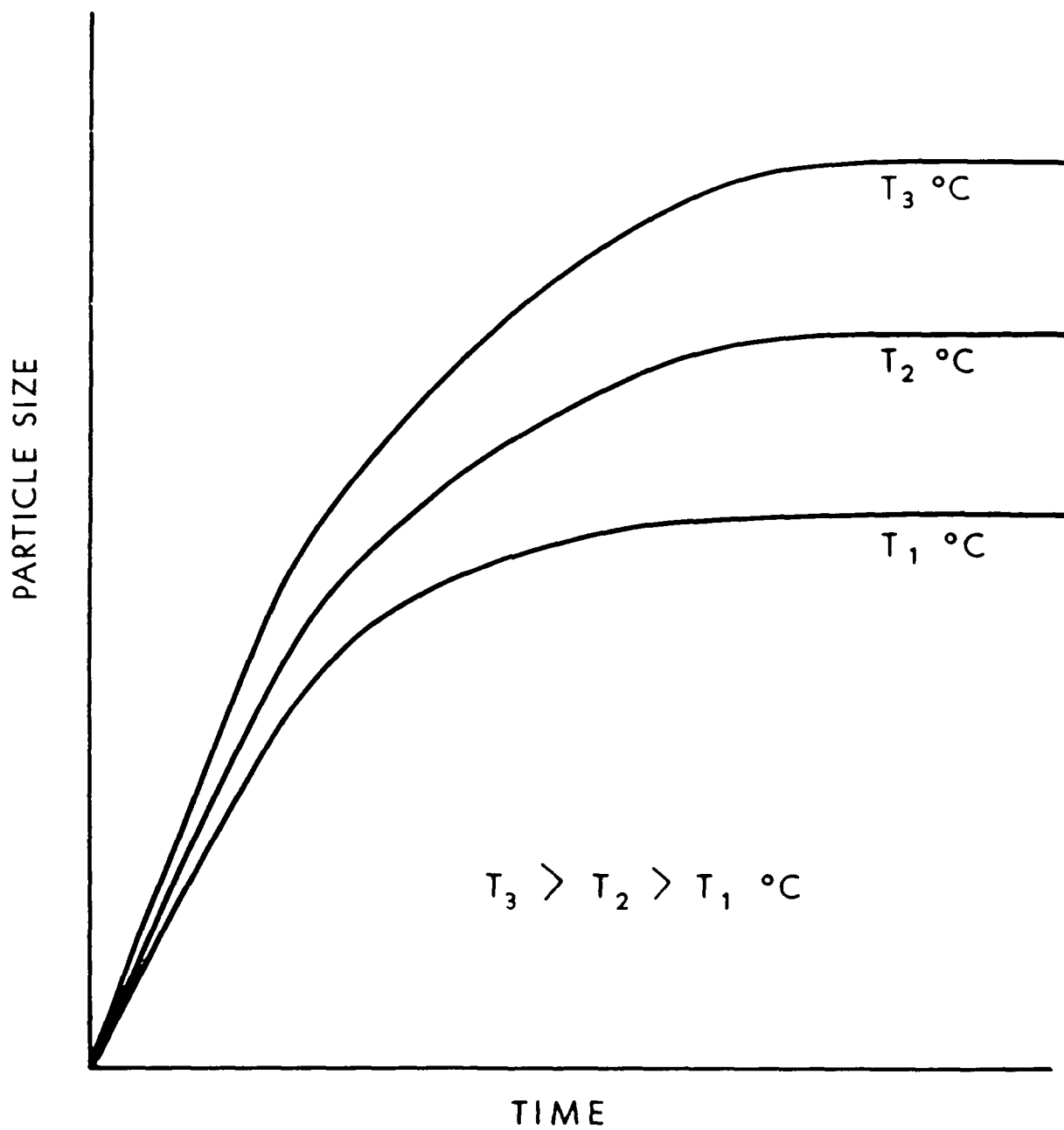
In order to disperse the colloidal sized oxide particles into the molten aluminum alloy as individual particles, it is necessary to keep the particles physically separated from each other prior to them actually being dispersed and wetted in the molten alloy. Failure to keep the particles physically separated from each other at the high melt temperatures, will cause the particles to agglomerate when they come into contact with each

other at the melt temperatures. The physical separation is accomplished by uniformly dispersing the particles into copper by a chemical precipitation technique described in U.S. Patent No 3,143,789 R. K. Iler, S. F. West, and P. C. Yates assigned to E. I. DuPont, 1964).

In addition to agglomeration, colloidal particles can grow by "Ostwald ripening". Small particles, being more soluble, dissolve and the soluble fraction deposits on the larger particles, which are less soluble. This kind of growth is shown in Figure 4. A discussion of the behavior of colloidal particles can be found in section 5, "Solubility of Colloidal Particles" and "Gel Structure". In the Phase I study, care was taken to avoid both types of particle growth.

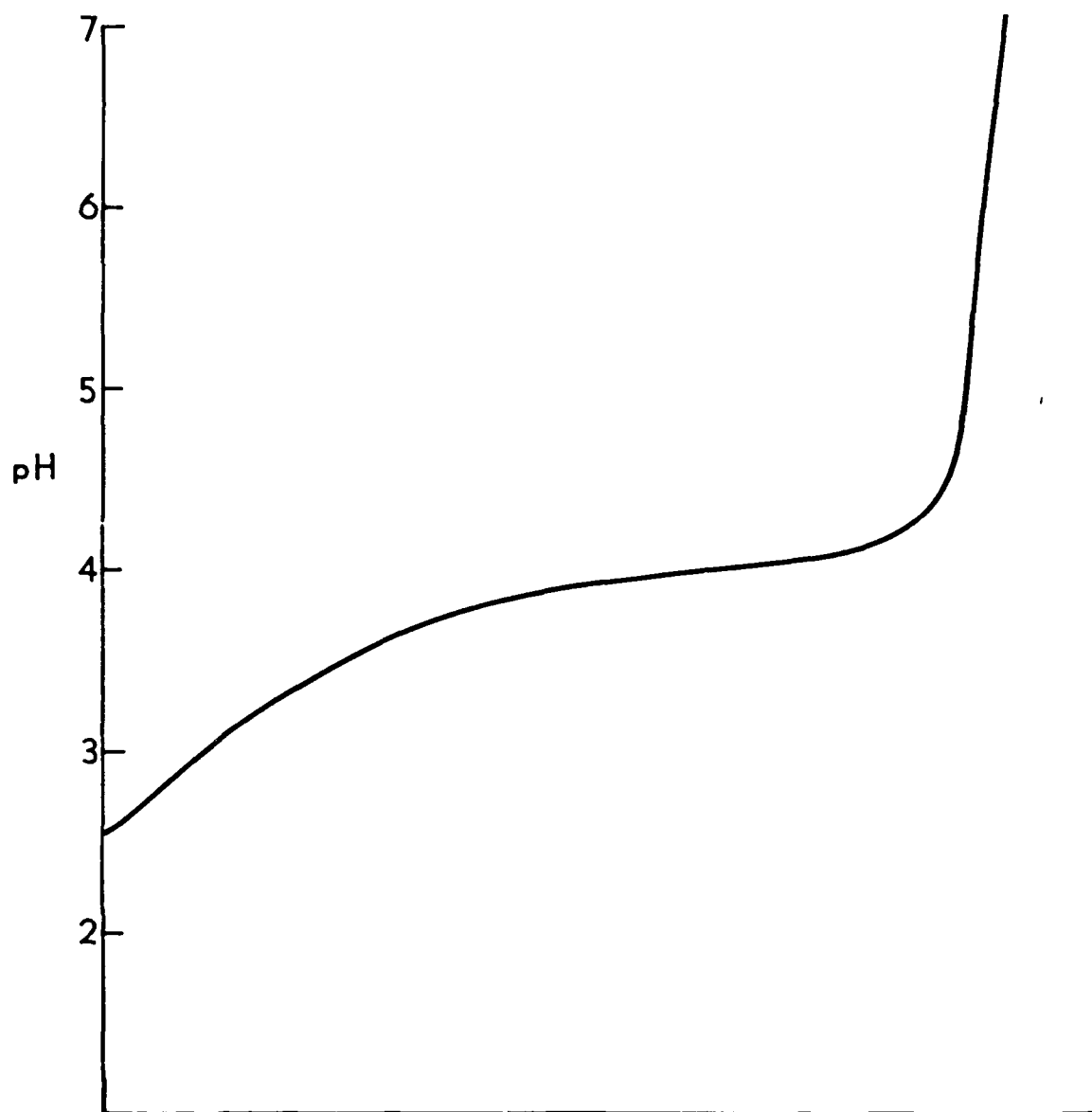
In the precipitation reaction, a solution of copper nitrate was precipitated as copper hydroxide by reaction with ammonium hydroxide. As the copper hydroxide precipitate forms, it essentially encapsulates the colloidal oxide particles which are present in the oxide sol. After reduction with hydrogen, the oxide particles remain uniformly dispersed through the metallic copper. When the copper is dissolved into the molten aluminum alloy, the oxide particles disperse individually into the molten alloy rather than agglomerating with adjacent particles.

A titration curve was developed in order to find the optimum conditions for precipitating copper hydroxide with ammonium hydroxide, as shown in Figure 5. As ammonium hydroxide was added to copper nitrate, a blue precipitate begins to form around a pH of 3. As the pH of the solution was raised above 7.5, the solution



PARTICLE GROWTH

FIGURE 4



Volume Ammonium Hydroxide Added

Copper Nitrate Titration Curve

FIGURE 5

turns a dark blue and the precipitate begins to dissolve as an amine complex. To determine the optimum pH for precipitation of copper from solution, the following test was performed. Three hundred grams of copper nitrate trihydrate was dissolved in distilled water, and water added to form 1 liter. Ammonium hydroxide was added until the solution pH was 7.0. The solution was filtered and the precipitate discarded. Additional copper nitrate solution was then slowly added to the filtrate, lowering the pH. It was observed that additional precipitate was formed as the pH was lowered to 5.7. The solution was again filtered, the precipitate discarded, and additional copper nitrate solution was added. As the pH was decreased to 4.3, no additional precipitate was formed. From this experiment it was concluded that the maximum copper precipitate forms at a solution pH of 5.7. All coprecipitation reactions were conducted at this pH.

4.1.3 OM Copper Dispersion Preparation

A coprecipitate of copper and colloidal oxide was prepared as follows:

A solution of copper nitrate was prepared by dissolving copper nitrate hydrate into distilled water. An oxide sol, prepared as in the previous section, was added to distilled water such that the resulting solution is the same volume as the copper nitrate solution. A third solution of ammonium hydroxide is prepared, the amount of ammonium hydroxide being in slight excess of what is calculated to be required to precipitate all of the copper nitrate. The three solutions are added to a mixer

volumetrically as shown in Figure 2. The rate of ammonium hydroxide addition is controlled as to maintain the precipitated solution pH in the mixer of 5.2 to 5.7.

The precipitated copper hydroxide containing the dispersed oxide particles is filtered and washed to remove any soluble salts. The filter cake is then dried in an oven, where it changes from the blue hydroxide to black copper oxide.

After the copper oxide has been prepared it is placed into quartz boats and loaded into a tube furnace, where a mixture of nitrogen and hydrogen is passed over the oxide to reduce it to metallic copper. The colloidal alumina or thoria, which is dispersed in the copper, is much more stable than copper oxide, and will not react with the gaseous hydrogen. The temperature of the copper reduction must be carefully controlled to prevent an uncontrolled reaction between the copper oxide and hydrogen. The furnace temperature was maintained at 200°C for 2 hours, and then increased to 400°C for another 2 hours. If the reduction takes place at much higher rates and temperatures, the heat from the reaction between the copper oxide and hydrogen will cause the surface of the powder to sinter, trapping unreducible copper oxide below the surface.

Mixtures of AM copper and TM copper were prepared by the above methods. The relative quantities of colloidal oxide sol and copper nitrate in the precipitation reaction were controlled so that the oxide was present at 10, 20 and 30 volume percent of the OM copper. Preparation of these mixtures on a volume basis allows a similar number of thoria and alumina particles

to be dispersed into the final aluminum alloy. Chemical analysis of the powders confirmed the proper concentration of oxide in the copper powder.

Another method of manufacturing the AM copper mixture was also evaluated. A solution of aluminum nitrate was added to the mixer simultaneously with the copper nitrate solution and precipitated with ammonium hydroxide. The aluminum hydroxide precipitated along with the copper hydroxide. The precipitate was then filtered, dried, and reduced as before. On both occasions that AM copper powder containing 20% alumina prepared by this technique was exposed to air, it became pyrophoric and oxidized very rapidly, indicating a very small particle size. Because of the difficulty in handling this material, extensive characterization was not attempted.

4.1.4 Aluminum

Two aluminum alloys were used to study the dispersion of copper/oxide mixtures into the molten alloy. The first was commercially pure aluminum, containing more than 99.7% aluminum, with iron and silicon as the primary impurities. The other was a commercial sand casting alloy, number 356. It contained 7% silicon, .3% magnesium, and lesser quantities of copper, iron, manganese and zinc.

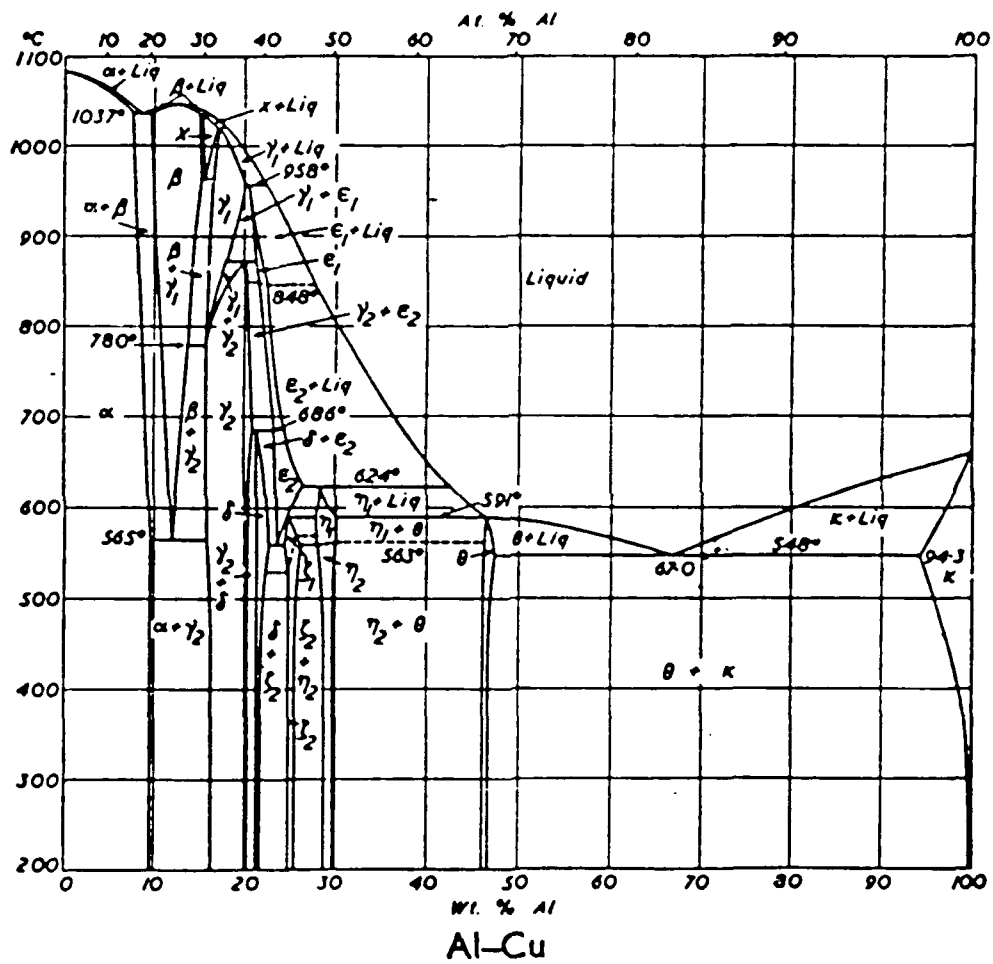
Attempts to use aluminum powder were not successful. The aluminum powder had such a high oxide content that the surface of the melt was covered with large quantities of alumina.

4.2 Results

4.2.1 Dispersion of OM copper Powder in Aluminum Melts

In order for the OM copper mastermix to be dispersed into the aluminum melt, a number of processes need to occur. First, the molten aluminum alloy must come in direct contact with the copper. Second, diffusion of aluminum into the copper must take place to the extent necessary to solubilize and dissolve the copper/aluminum mixture into the molten aluminum alloy. As can be seen from the phase diagram in Figure 6, the addition of 30% by weight aluminum must diffuse into the copper before the copper/aluminum compound becomes liquid at the melt temperature, 800° C. Third, magnesium in the molten aluminum alloy reacts with the colloidal oxide particles rendering them metallophillic or wet by the molten aluminum alloy.

Initial tests were performed by simply sprinkling the TM copper powder on the surface of the molten aluminum alloy, to which 1% magnesium had been added. The powder floated on the molten aluminum surface. Stirring with a graphite rod resulted in some powder sticking to the rod, while another portion sank to the bottom of the crucible containing the melt. Variations of temperature from 800° to 900° C, and contact times between the powder and the molten aluminum from one half to one hour revealed no reproducible conditions under which a majority of the powder would disperse into the molten aluminum. Variations of thorium content, magnesium content, and using alumina in the place of thorium likewise resulted in a majority of the powder not dispersing into the molten aluminum. Powders which were



Phase Diagram
Metals Reference Book, C. J. Smithells
3rd Ed, Vol. 1, Batterworths, 1962

FIGURE 6

exposed to atmospheric oxygen were compared to those which had been maintained in either an argon or nitrogen atmosphere, again unsuccessfully.

Copper powder which was prepared in the same manner as the OM mixtures was placed in the aluminum melt under the same conditions as the OM mixtures. Quantitatively, more of the powder went into the molten aluminum when the oxide was absent, however, some of the copper could still be recovered as a fine powder after the melt has been poured.

As these tests progressed, it became apparent that the molten aluminum alloy was not wetting the surface of the copper. After finding that the atmosphere in which the melt was taking place seemed to have no effect on improving this wetting, the oxide powder was placed into a piece of aluminum foil in order to increase the time that the powder was in the center of the melt, surrounded by molten aluminum alloy, rather than resting on the surface or at the bottom of the crucible. This approach yielded no better results.

4.2.2 Dispersion of OM copper Pellets in Aluminum Melts

To reduce the surface area of the AM copper or TM copper, the powder was pressed in a hydraulic press into pellets or slugs approximately 25 cm dia. and 2 mm thick. After pressing the pellets, they were again reduced in a hydrogen atmosphere to remove any copper oxide which may have formed during the pressing operation.

After the aluminum was melted and brought to temperature,

magnesium was added, and the melt periodically stirred for 5 minutes. The pellet was then carefully dropped into the melt. Depending upon the colloidal oxide concentration, the temperature of the melt, and the magnesium content, the pellet would dissolve in 10 to 30 minutes. The melts were maintained at temperature for a total of 30 to 60 minutes after the pellet was added to the melt. Chemical analysis of the aluminum alloy containing the dissolved pellet confirmed that the pellet had dissolved. Experiments with both chemically pure aluminum and the 365 casting alloy confirmed that the copper pellets could be dissolved in a range of aluminum alloy compositions.

In order to determine the optimum conditions for dissolving the OM copper pellet into the aluminum melt, a computer optimized experimental design was conducted. The experimental design and results are shown in Table 1. From this series of experiments, the optimum conditions to dissolve the OM copper pellet are high temperature (950°C), long melt times and high magnesium contents. From a practical standpoint, pellets containing 10 to 20% by volume of dispersed oxide can be dissolved into an aluminum melt containing from 1 to 6% by weight magnesium. In those experiments in which a part of the pellet was found after the melt was poured into a separate container, a cross-sectional examination of the pellet revealed that sufficient aluminum had not diffused into the copper to render it soluble.

4.2.3 Oxide Wetting Studies

A potential alternative method of dispersing the oxide

TABLE 1

COPPER/OXIDE PELLET DISSOLUTION EXPERIMENTS

<u>Experiment Number</u>	<u>Temp. °C</u>	<u>Time</u>	<u>Fill Type</u>	<u>% Fill (1)</u>	<u>% Mg (2)</u>	<u>Pellet Dissolve?</u>
1	800	20.		0.	6.	
2	800	20.		0.	3.	
3	900	60.	3	20.	3.	
4	800	60.	3	20.	6.	
5	900	30.	3	20.	6.	
6	800	30.	1	10.	3.	NO
7	800	60.	1	10.	6.	
8	900	30.	1	10.	6.	
9	900	60.	2	10.	6.	
10	900	60.	1	20.	6.	
11	900	30.	2	10.	3.	
12	900	60.	3	10.	6.	
13	800	60.	3	10.	3.	
14	800	60.	2	20.	3.	
15	800	30.	2	20.	6.	NO
16	900	60.	1	10.	3.	
17	800	30.	1	20.	3.	NO
18	900	30.	2	20.	3.	NO
19	900	60.	1	20.	3.	
20	800	60.	3	10.	3.	
21	800	60.	1	20.	3.	
22	900	30.		0.	1.	
23	900	60.	3	10	1.	
24	900	60.	2	10	1.	

Legend

Fill Type 1 - Alumina From Commercial Source

Fill Type 2 - Alumina From Aluminum Nitrate Precipitation

Fill Type 3 - Thoria

(1) Volume Percent la Copper Pellet

(2) Weight Percent Magnesium la Final Alloy

particle in the aluminum melt is to add the oxide directly to the molten aluminum. Oxide of calcium, magnesium, zirconium, and aluminum were added to the surface of the molten aluminum alloy. The oxides were not wet or dispersed into the molten alloy, probably for the same reasons that the OM copper powder did not disperse. Vigorous agitation of the aluminum melt may have caused more dispersion and wetting, however, the probability of the colloidal sized oxide particle aggregating is high using this dispersion technique.

4.2.4 Microscopic Examinations

Figure 7 is an electron micrograph of the alumina which has been dispersed in water to form the sol. The particle size ranges from 10 to 40 millimicrons. The particle size range is satisfactory for oxide dispersion strengthening from a theoretical standpoint.

Figures 8, 9 and 10 are transmission electron micrographs of foil samples of the aluminum alloy. These pictures were taken by Mark Plichta, University of Utah. In all three figures, the aluminum alloy is of identical alloy composition, containing 4% copper and 3% magnesium as the only major alloying agents.

Figure 8 is of the control, containing no dispersed oxide. In this alloy, a copper/aluminum intermetallic precipitate is readily apparent. It is this intermetallic component which gives aluminum alloys containing copper their heat treatability and strengthening characteristics. As can be predicted from the phase diagram shown in Figure 6, the majority of the copper



FIGURE 7
T. E. M. 100,000X
 Al_2O_3 Sol.



FIGURE 8

Al - 4 Cu - 3 Mg Control
13000X

Note: Intermetallics, grain boundaries



FIGURE 9
ODS Aluminum 15000X
Al - 4 Cu - 3 Mg
.004 Volume % Alumina

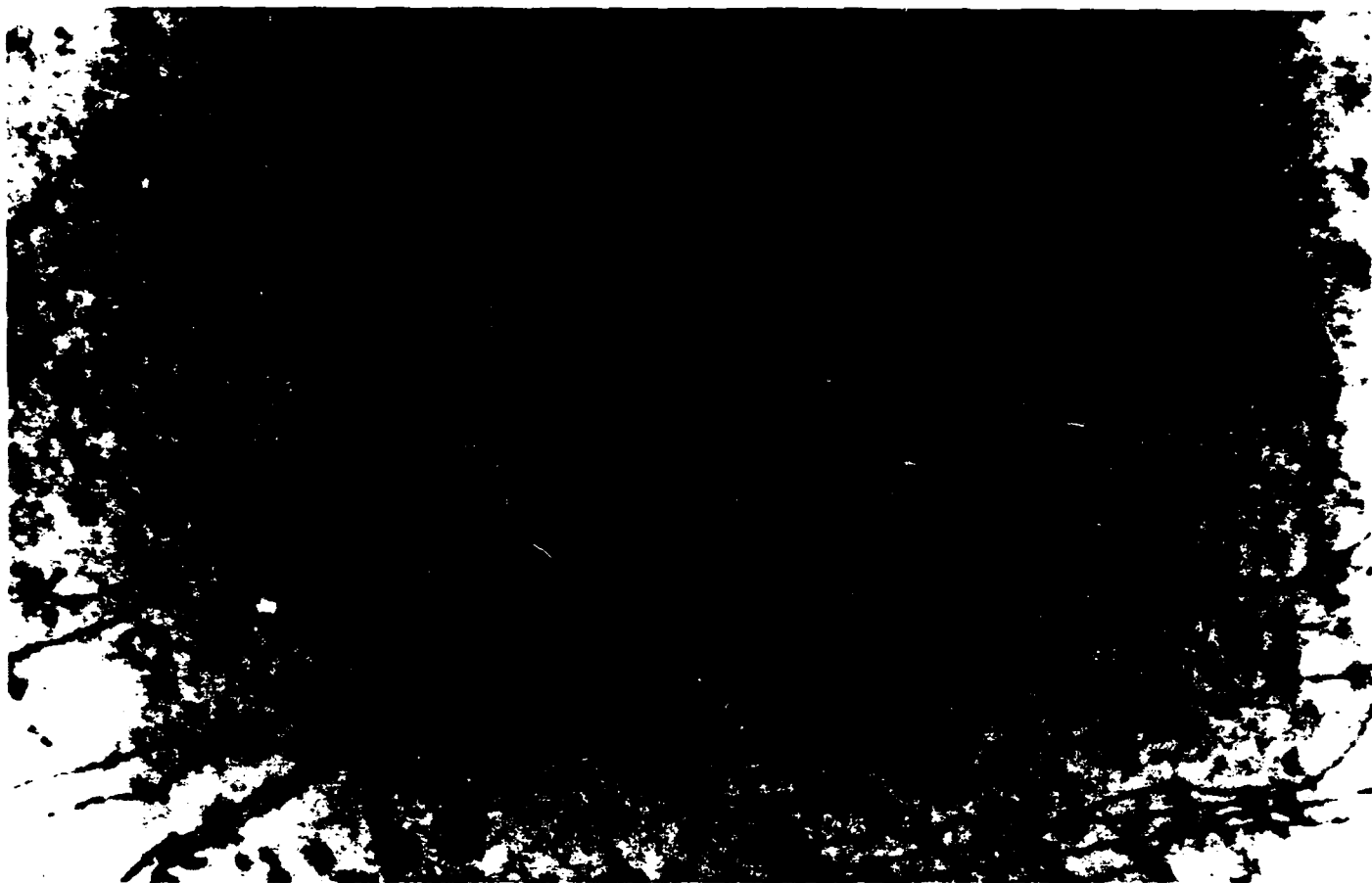


FIGURE 10
ODS Aluminum 100000X
Al 4 Cu 3 Mg

in a high copper alloy is not soluble at room temperature, leading to these precipitates.

In Figure 9, the dispersed alumina oxide is readily apparent. The dispersion is uniform throughout the sample. Because this is a transmission micrograph of the actual sample, the particles appear much closer than they are if the sample thickness of about 300 millimicrons.

Figure 10 is a higher magnification view of the same sample shown in Figure 9. The individual particles closely resemble the size and shape of the original alumina particles shown in Figure 7. Because the particles are approximately the same size as the sol prior to dispersion in the melt, it is apparent that no substantial agglomeration occurred during processing.

Figures 11, 12 and 13 are micrographs prepared by carbon replication of the aluminum alloy surface by Micron, Inc., Wilmington, Delaware. Figure 11, being the control, shows no surface indication of any dispersed oxide. Figure 12 is an aluminum melt containing thoria. In preparation of the sample, the individual thoria particles were extracted from the aluminum alloy, indicating that the thoria particles are poorly wet in the aluminum alloy. Other micrographs both of carbon replicas as well as transmission micrographs of the actual aluminum sample indicate that the thoria preferentially concentrates along grain boundaries and in the intermetallic copper/aluminum particles. As the aluminum alloy solidifies, the thoria is rejected and concentrates in those regions which are the last to solidify.

Figure 13 is a replica of an alumina containing alloy.



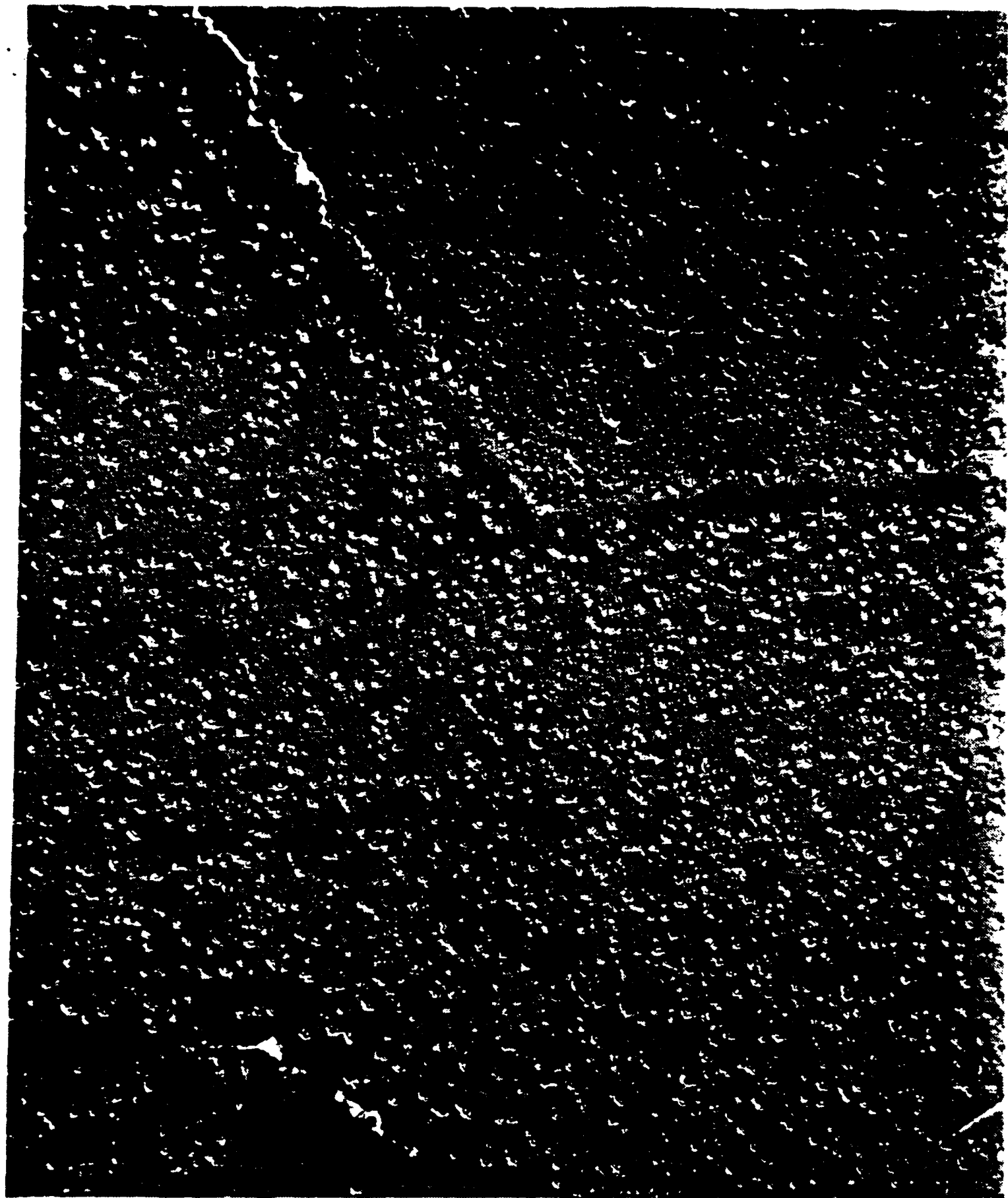
TEM 10,500X
CONTROL SAMPLE

Figure 11



TEM 10,500X
DISPERSED THORIA SAMPLE

Figure 12



TEM 10,500X
DISPERSED ALUMINA SAMPLE

Figure 13

There is no evidence of the alumina particles being concentrated along the boundaries nor are they extracted in the carbon replication process. It appears that the intermetallic phase may be precipitating around the alumina particles.

4.2.5 Physical Property Measurements

As shown in Figure 3, aluminum alloy prepared from casting alloy 356 to which was added magnesium and copper, an increase in room temperature hardness was observed both after casting and after annealing following cold working in the sample containing an alumina oxide dispersion. Although this result may indicate some room temperature hardness improvement by adding oxide to the aluminum alloy, more significant measurements may be made at high temperature.

Because the level of copper in this alloy is above the solubility limit of copper in aluminum at room temperature, heat treatment may result in the precipitation of intermetallic compounds which also have a marked effect on room temperature hardness measurements. It may be successfully argued that the room temperature hardness improvement may be more a function of the precipitation of intermetallic phases, and any contribution as a result of the oxide dispersal to strength improvements at room temperature may be completely masked. Therefore, meaningful physical property measurements must be conducted in the absence of any intermetallic precipitate. These measurements may either be made on the same alloy at high temperatures where the copper is soluble, or by reducing the copper concentration. These

tasks remain to be accomplished in Phase II.

4.2.6 Discussion

The failure of the OM copper powder to disperse into the aluminum melt may be a function of a number of variables. The powder may be contaminated with a small quantity of copper oxide. The powder may have a portion of its surface as the colloidal oxide particles, which may inhibit wetting and dissolving of the copper. Or the molten aluminum alloy may have interfacial tension characteristics which prevent it from effectively displacing gas from the surface of the solid OM copper particles. When the powder is pressed into a pellet, the surface area may be reduced to such an extent that once the molten aluminum has finally displaced gas from the surface of the OM copper diffusion of aluminum into the copper and solution of the pellet may proceed. Another method of dispersing the OM copper powder into the molten aluminum alloy may be through very high agitation, such as through ultrasonics to aid in the initial wetting of the OM copper surface. This approach has produced favorable results by others dispersing larger particles.

5. Discussion of Results

5.1 Fundamentals

In section 4.1.2 reference was made to the various type of growth which can occur in colloidal systems, including Oswald ripening and gelation.

The discussion which follows is intended to cover these

principles in colloidal chemistry, and particularly those which could apply during the preparation of the AM copper master alloy slugs and/or during the dispersing of alumina from such a master alloy in a molten aluminum alloy. In this discussion, silica is used as a model system. The discussion includes:

- solubility of silica in water
- colloidal particle growth as a result of solubility
- gelation or aggregation
- coalescence of gels.

In the aluminum-copper-alumina system, the analogy is:

- alumina has solubility in copper and or copper-aluminum
- alumina particle growth can occur, which in turn decreases IPS
- in AM copper, gelation and coalescence can occur which also decreases IPS

IPS is the key to dispersion strengthening. Unless the factors which control IPS are controlled, the system is out of control. The P.I. of this project is fully conversant with IPS and how to control it. Without that knowledge the development of a successful ODS aluminum will be very difficult indeed.

5.1.1 Solubility of Colloidal Particles.

A. The solubility of colloidal particles in any solvent can be illustrated by the solubility of silica in water. Monosilicic acid, H_4SiO_4 , is a very weak acid and may be present in water to the extent of about 0.05%. It is readily detected by reaction with molybdic acid (1). If present in higher concentrations, monosilicic acid will polymerize, first to disilicic acid, then

polysilicic acid, and finally to amorphous silica. All of these polymers of silica are in equilibrium with a small but definite amount of monosilicic acid (2).

The effect of particle size (or surface area) on the solubility of silica is shown in figure 14, the effect of pH in figure 15 and the mechanism for growth of amorphous silica particles is shown in figure 16.

Any group of amorphous silica particles of a given size in water is in equilibrium with a fixed amount of monosilicic acid (2). In general the larger the particle, the smaller will be the amount of monosilicic acid in equilibrium with the particle. Silica particles in water grow by the mechanism of the smaller particles dissolving to produce monosilicic acid, and this monosilicic acid then deposits on the larger, less soluble particles (2).

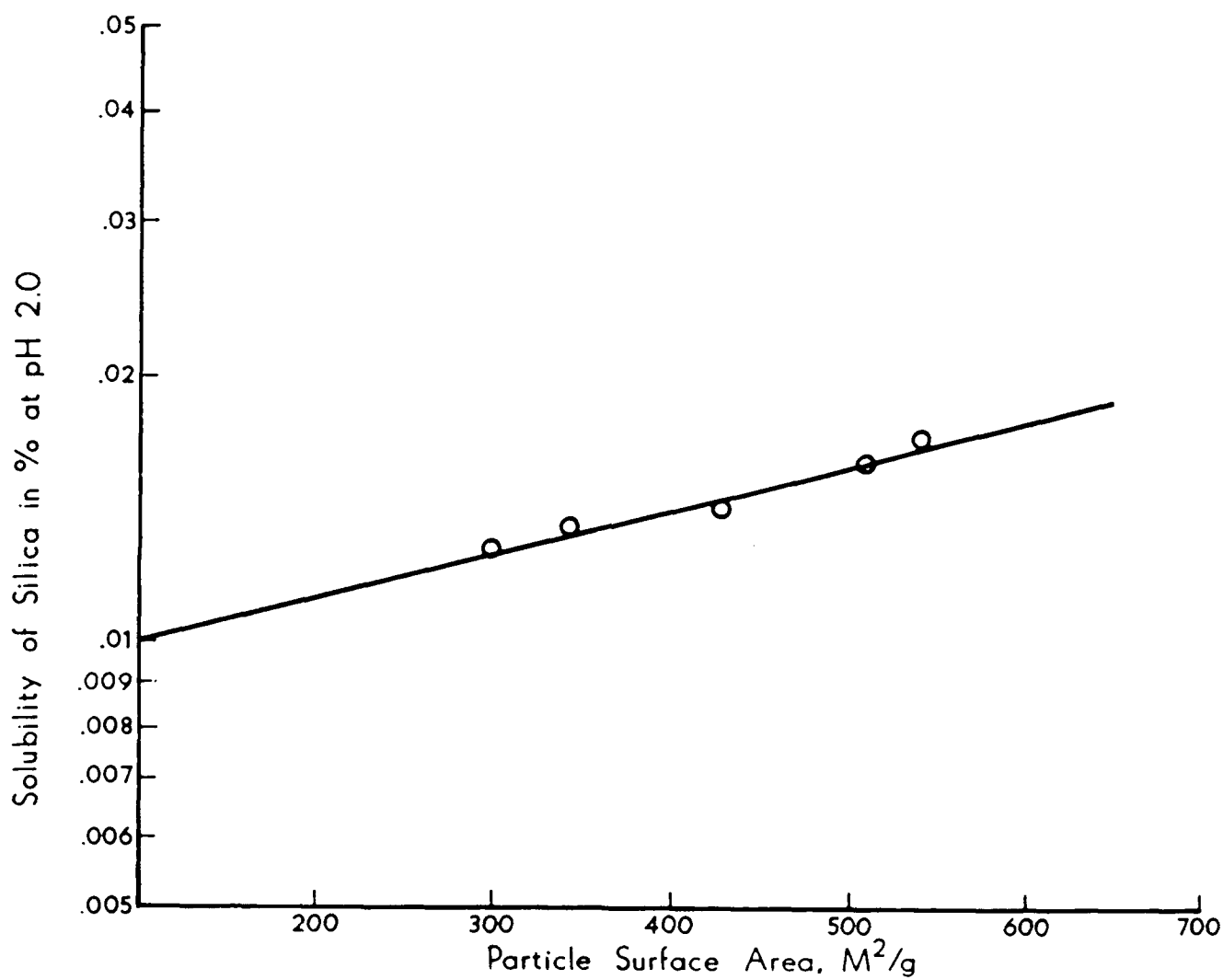
The surface energy for amorphous silica colloids in water is given by the relationship:

$$\frac{RT}{M} (\ln) \left[\frac{S_r}{S} \right] = \frac{2E}{dr}$$

where: R = constant, cal/degree/mol
 T = absolute temperature, degrees
 M = molecular weight, g
 S_r = solubility of particle of radius, r
 S = solubility of a massive particle, cm
 d = density of the particle, gm/cc
 E = surface energy in calories/sq cm

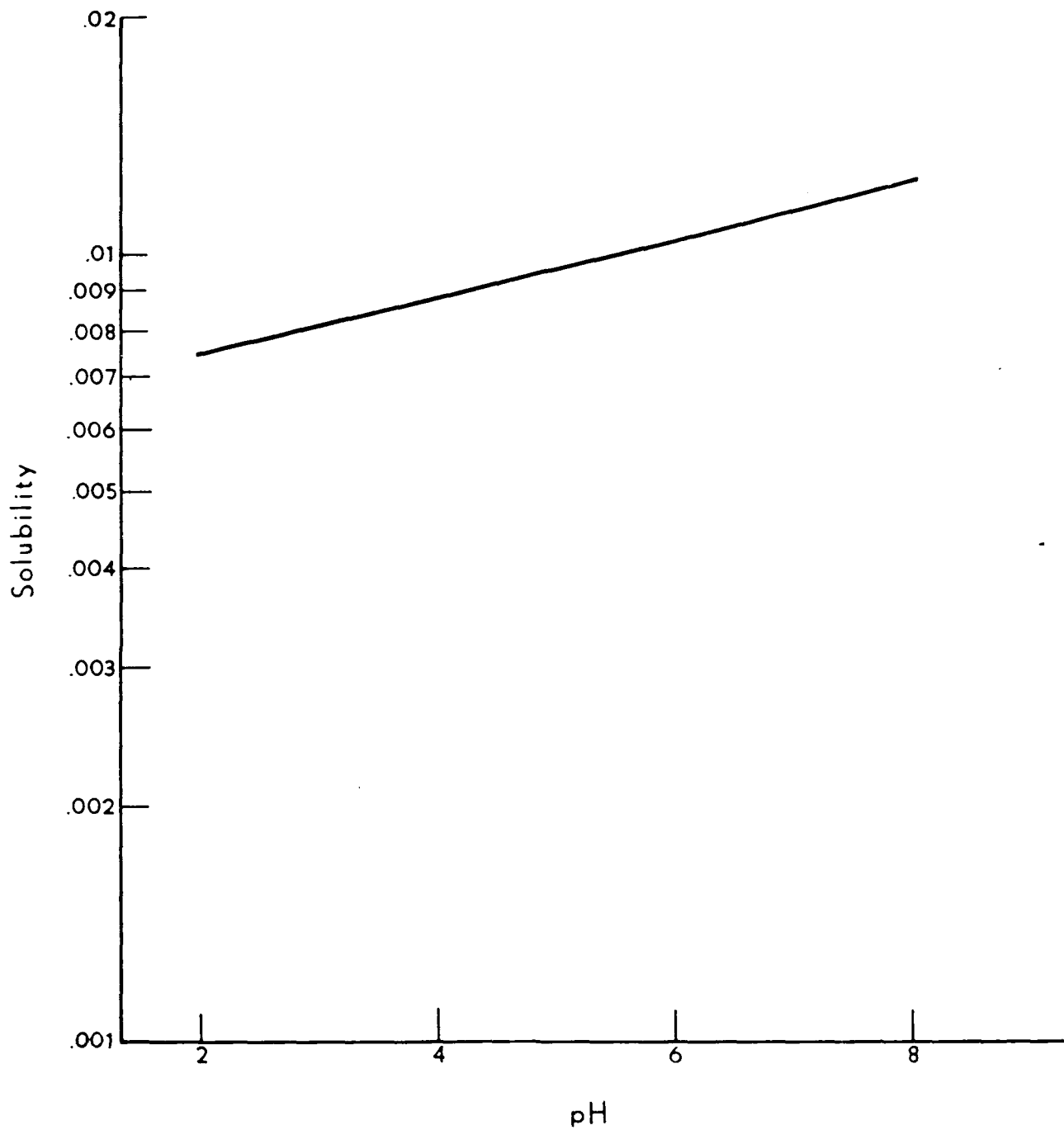
For amorphous silica
 E = 1.1x10⁻⁶ Cal/cm

B. Research at the DuPont Company (4) has shown that the same principle applies to the solubility of colloidal oxide



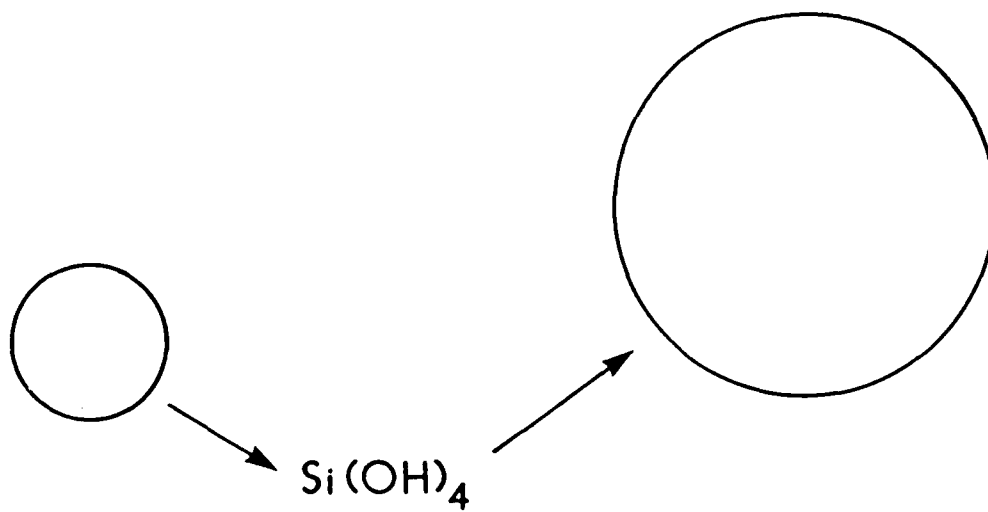
SOLUBILITY OF SILICA IN WATER

FIGURE 14



SOLUBILITY OF SILICA VS pH

FIGURE 15



COLLOIDAL PARTICLE GROWTH

Small particles have a higher solubility than large ones. Small particles dissolve and the silicic acid deposits on the larger particles.

FIGURE 16

particles in metals. Silica has a solubility in copper, silicon atoms and oxygen atoms migrating through a copper matrix, and as temperature is increased 20 millimicron silica in copper grows, such that at about 800° C, and about 24 hours, they reach a size approaching 1 micron. Growth rate curves are shown in Figure 4.

Dispersions of metal oxides in copper were prepared and subjected to an 800 C anneal (4). Particle growth occurred as follows:

<u>Oxide</u>	<u>Size after 800° C</u>
SiO ₂	1000 millimicrons
TiO ₂	250
ZrO ₂	100
Al ₂ O ₃	50

The growth correlation appears to be related to the free energy of formation of the oxide in question, the more negative the free energy, the more stable are the colloidal size particles in copper, i.e., the lower the solubility at temperature. In the ODS aluminum system, temperatures of the cast alloy certainly will not be hot enough for particle growth to occur, and since the colloidal particles in the castings approach the particle size of the starting alumina in the coprecipitate, it appears that very little particle growth occurred in the melt.

5.1.2 Gel Structures

If one starts with monosilicic acid in water in concentrations greater than the solubility limit, polymerization will occur in one of two ways:

- a) Spherical amorphous silica will form and continue to

grow in size in a spherical shape until the solubility requirements are satisfied. This type of growth tends to occur in alkaline solutions containing little or no dissolved salt. In such solutions the amorphous silica particles take on a negative charge due to "absorption" of silicate ions, $\text{Si}(\text{OH})_3^-$. On the other hand, in the presence of acid and or dissolved salts, there is a tendency for gels to form. See Figure 17 (3). When two particles come together to form a gel, there is a tendency for monosilicic acid to deposit in the crevice of the gel, because of the negative radius of the curvature. Figure 18 (3).

In the preparation of the copper-alumina master batch, one must be careful to avoid aggregation because this will, in effect, create big particles from small ones, and increase the IPS (interparticle spacing) and decrease the dispersion hardening effect (See below). Principles learned from silica polymerization were applied to the development of the process of ODS Aluminum.

5.1.3 Interparticle spacing

In the system alumina-copper, the effect of the dispersed particle (alumina) on the properties of the matrix (copper) is a function of interparticle spacing. One effect occurs because the dispersed particle blocks the movement of dislocations (6-8). Dispersed particles also prevent grain growth. The overall effect is a function of:

- a) interparticle spacing and
- b) dispersed particle size.

Interparticle spacing can be calculated by the relationship:

Aggregate Formed From
Discrete Particles

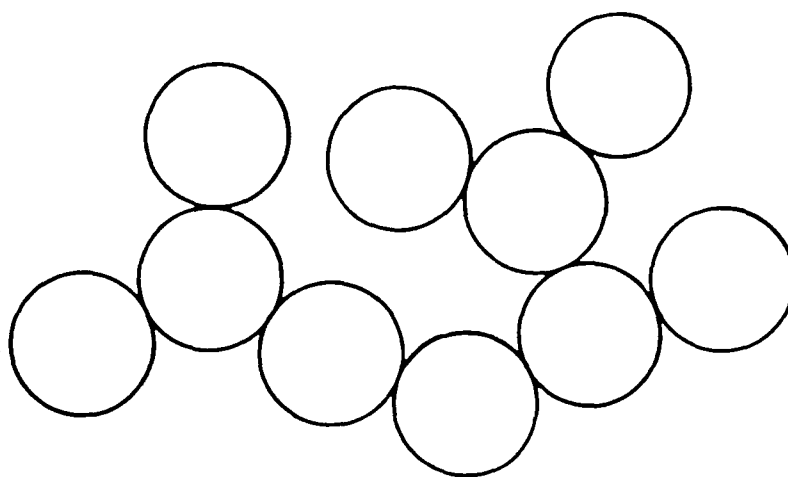


FIGURE 17

Coalescence Causes Necks Between Particles
To Coarsen

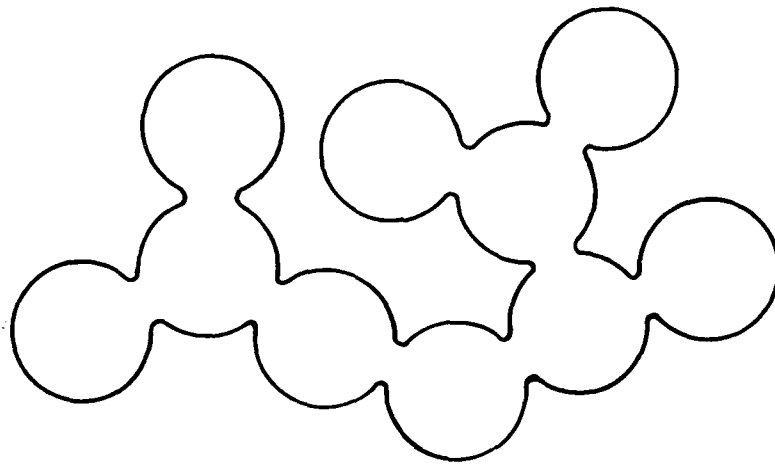


FIGURE 18

$$I = d \left[\left(\frac{1}{1.91f} \right)^{1/3} - 1 \right]$$

Where

I is the interparticle spacing

d is the particle diameter, same unit as I

f is the volume fraction of the particle

Empirically it was shown (9) that grain size of a metal containing dispersed oxide particles is approximated by the relationship:

$$G = \frac{0.37d}{f}$$

5.1.4 Summary

To control the effect of dispersed oxides in metals one needs to control:

- a) solubility of particles in a matrix
- b) gelation, coalescence and resulting particle growth
- c) interparticle spacing and its effect on grain size and dislocation migration.

Bibliography - Section 5.1

1. G. B. Alexander, "The Reaction of Low Molecular Weight Silicic Acid with Molybdic Acid," JACS, 75: 5655 (1953).
2. G. B. Alexander, W. M. Heston and R. K. Iler, "The Solubility of Amorphous Silica in Water," J. Phys. Chem. 58: 453 (1954).
3. Unpublished data, Industrial and Biochemicals Department, E. I. duPont de Nemours and co.
4. P. C. Yates, private communication.
5. G. I. Taylor, Proc. Roy. Soc. A145. 362 (1934).
6. E. Orwan, Zeit. Phys. 89: 605, 614, 634 (1934).
7. M. Polanyi, Zeit. Phys. 89: 660 (1934).
8. G. B. Alexander, R. K. Iler, S. F. West, US 2,972,529, Column II, February 21, 1961.

5.2 TD Nickel

A discussion of TD Nickel is included in the Phase I report so that a projection from TD Nickel to ODS aluminum can be made. The properties of TD Nickel are described in a product bulletins of DuPont and Fansteel (1, 2), in Metal Progress, "A Dispersion-Strengthened Nickel Alloy" (3) and in an impact report, "Tiny Particles Turn Metals into Superperformers" (4). See also, "An Investigation of a New Nickel Alloy Strengthened by Dispersed Thoria" (5) and "A Microplasticity Study of Dispersion Strengthening in TD-Nickel" (6), and "Coated TD Nickel" (7).

The following is extracted from the Metal Progress article:

A new nickel alloy, containing 2% thoria as an insoluble second phase, offers high temperature stability and useful mechanical properties virtually to the melting point of the base metal. It is easy to fabricate and has a wide forging range.

Strengthening alloys with small particles of a second phase in the microstructure is one of the most powerful techniques used by metallurgists and is a major factor in increasing the mechanical properties of many structural alloys. There are two methods of producing the small particles. In the more common method, carefully selected metal compositions are heated in such a way as to dissolve and then precipitate, in a controlled manner, the particles of second phase; this will be referred to as "precipitation hardening." The less common method, employed in making TD nickel, involves adding a second phase in the form of fine particles which remain inert and relatively insoluble throughout the process; this will be called "dispersion strengthening".

A freedom of choice exists in the design of dispersion-strengthened alloys which does not exist in precipitation-hardened material. In principle, one can choose an inherently insoluble, stable second phase for dispersion strengthening, whereas it is a requirement of precipitation-hardening systems that the second phase be more soluble at higher temperatures. This limits the temperature at which maximum strength can be obtained. In contrast, the strength of TD-type alloys does not depend on heat treatment . . .

Figure 19 shows the microstructure of drawn bar stock, 3/4 in. in diameter of TD Nickel. Many of the thoria particles in the nickel were extracted during preparation of this electron micrograph. In most instances, they appear as individual spherical particles 0.1 micron in diameter or smaller . . .

Considering only strength, one would tend to add greater and greater quantities of this second phase, providing, of course, particle size and distribution can be maintained. Fabrication and ductility requirements forced a compromise, however. First it was established that the strength of nickel containing thoria particles 0.1 micron in size increases rapidly as the amount of oxide approaches 1 vol. %. Beyond this, strength improves at a much slower rate, and the loss of ductility is virtually proportional to the amount of second phase. The compromise--2% thoria--insures a good strengthening effect and adequate ductility.

Incorporating 2% thoria in pure nickel has very little effect on the physical properties. Unlike the superalloys, the melting point and the thermal and electrical conductivity remain high--essentially equivalent to nickel of the same purity. Some of the physical properties of TD nickel are shown in Exhibit 20, Table 1. The fabricability of TD Nickel is excellent. It can be converted and fabricated with high yields. There is no narrow forging temperature range. Forging can be done between room temperature and 2200 F, although intermediate and low temperatures are probably most useful. The alloy is readily machined, drawn and rolled. Mechanical properties, measured on bar stock, are given in Fig. 2. (Exhibit 20).

The yield strength decreases slowly from 50,000 psi at room temperature to 10,000 psi at 2400 F. This low degree of temperature sensitivity is also demonstrated by the creep and stress-rupture properties. See Exhibit 20.

Stress-rupture data (Fig 3 Exhibit 20) are reported on a modified Larson-Miller plot. The material constant, C, in the expression $P = T(C + \log t)$ was determined by the method of least squares using stress-rupture data over the temperature range 2600 to 2400 F and rupture times from 10 to 706 hr. This presentation of stress-rupture properties fits scores of test values with an accuracy of $\pm 10\%$. The high material constant, 34, indicates the stability of the alloy. Test temperature affects rupture strength most; strength is largely independent of time. We discontinued the tests after 700 hr at 2200 F at 6800 psi. (Exhibit 20).

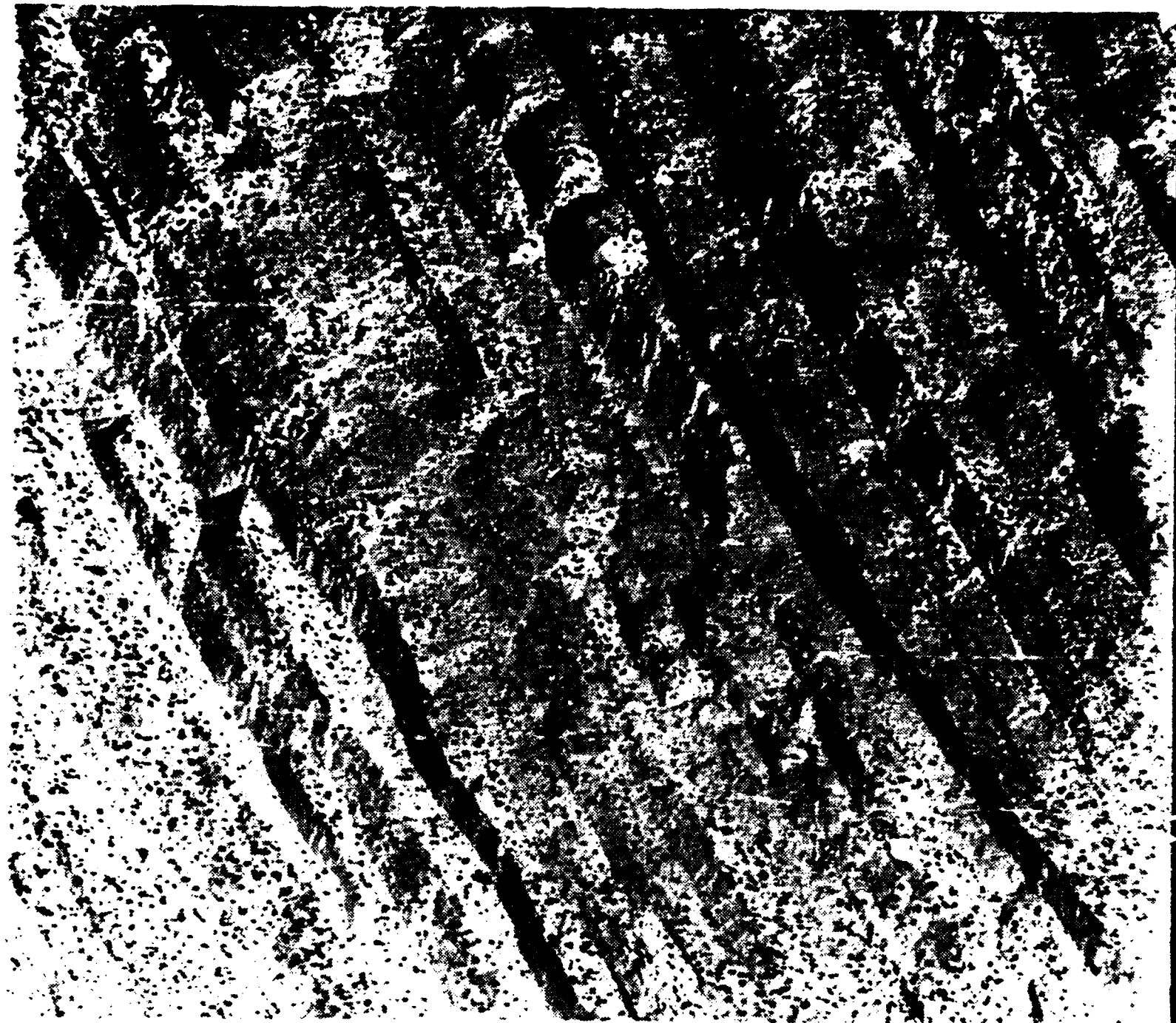


FIGURE 10

TD Nickel 9600X

Note: Extrusion lines, grains, thoria
distribution, IPS \sim 0.3 Microns

Table I — Comparison of Physical Properties

	TD Nickel	Nickel 200
Melting temperature, °F	2600	2615
Density, lb/cu in	0.322	0.321
Thermal conductivity at 70 F, Btu-sq ft/hr/°F-in	600	390
Electrical resistivity, microhm-cm	7.6	9.5
Mean coefficient of thermal expansion at 70-1500 F, per °F	8.3×10^{-6}	9.1×10^{-6}
Specific heat, Btu/lb/°F	0.106	0.109
Emissivity (2000 F)	0.65	0.60
(2400 F)	0.72	0.90

Table II — Mechanical Properties of TD Nickel

Fatigue strength (10 ⁷ cycles)	
Room temperature (mean stress = 0)	
Unnotched	45,000 psi*
Notched, K _t = 2.1	45,000*
1800 F (mean stress = alternating stress)	
Unnotched	5,000*
Impact strength, V-notch Charpy	
Room temperature	30 ft-lb
1800 F	30
Thermal shock resistance (wedge specimen)	
Oxyacetylene flame; air blast	500 cycles,
Flame, 10 sec to 2000 F	no failure
Air blast, 20 sec to 200 F	

*Alternating stress.

Table III — Corrosion Resistance of Several Nickel Alloys

	Weight Change, mg per sq cm		
	TD Nickel	Inconel "X"	Nickel 200
Fused Salts			
PbSO ₄ , 1650 F, 4 hr	1.1	22.8	8.5
1700 F, 4 hr	1	94	
PbBr, 1400 F, 1 hr	-7.7	-14.0	Badly corroded
90% Na ₂ SO ₄ , 10% NaCl, 1550 F, 6 hr	101	860*	129
Acids			
Conc HNO ₃ , RT, 50 hr	120		200
1/2 conc HNO ₃ , RT, 50 hr	200		450
Conc HCl, RT, 50 hr	115		115

*Hastelloy X.

Fig. 2 — Effect of temperature on the tensile properties of TD nickel bar stock is shown. A notch-tensile curve for mildly notched specimens is also included.

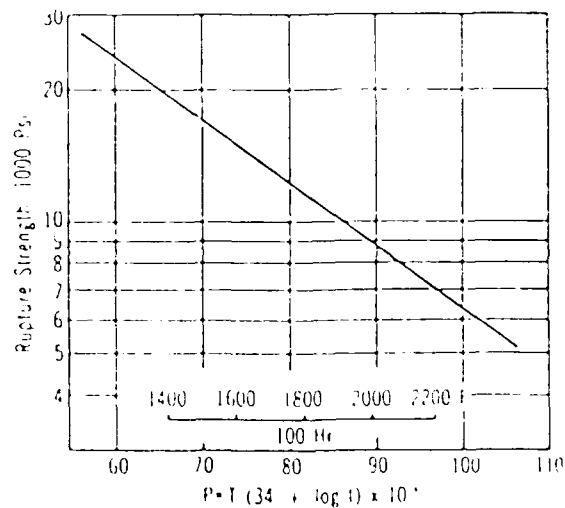
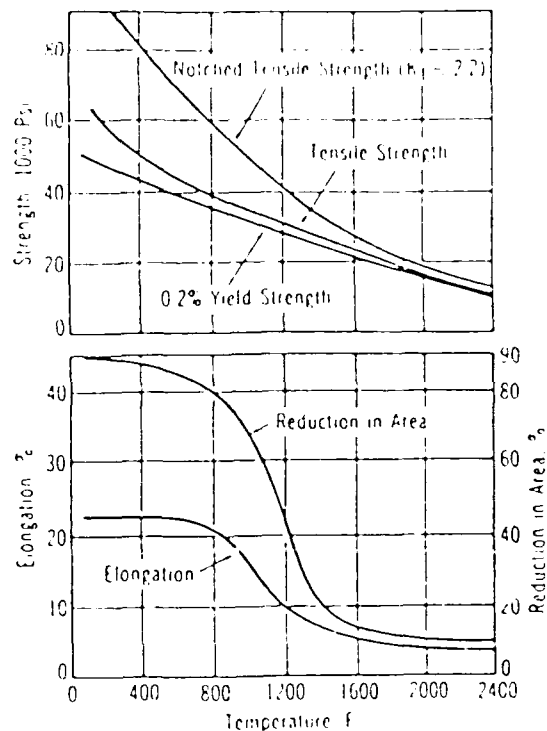


Fig. 3 — Stress-rupture data for TD nickel, presented on a Larson-Miller basis, indicate that strength depends largely on test temperature.

Table II, Exhibit 20, illustrates other mechanical fatigue characteristics, undoubtedly due to lack of stringing of the dispersed thoria. Uniform distribution of thoria imparts a high degree of toughness and virtually eliminates notch sensitivity.

Over the temperature range 1800° to 2400° F, TD nickel scales at a rate which is about three to five times slower than commercial wrought nickel. Of great interest is the lack of intergranular attack by oxidation. This is often observed in nickel alloys at temperatures above 2000° F. After exposure for 100'hr at 2200° F, TD nickel has no intergranular attack.

The entire loss of load-carrying ability as a result of oxidation may be calculated on the basis of the parabolic scaling constant shown in Fig. 5 (Exhibit 21). This predictability is unusual in the high-temperature field (above 2000 F) and most certainly will require serious consideration in design studies. Table III lists some corrosion data of TD Nickel compared to nickel, Inconel "X" and Hastelloy X.

From its earliest inception, TD nickel was designed for high-temperature service. Static exposure-stability tests conducted on the alloy demonstrate that the properties of the material are substantially unchanged, even after exposures of 2400° F for 1 hr (Fig 6, Exhibit 21). In addition to the fact that TD nickel retains substantial strength above 2300° F, its insensitivity to exposure at 2400° F insures the user that momentary overshoots in temperature will not affect the properties of the alloy on return to a lower service temperature.

The stability of any alloy has a profound influence on joining techniques. When precipitation-hardened superalloys are brazed, it is imperative that the braze cycle be compatible with the heat treating sequence for the alloy. This often limits brazing temperatures. The stability of TD nickel permits it to be brazed with alloys having high melting points, and the thoria does not interfere with wetting of the braze metal.

Welding presents a different type of problem. Although there is inherently no problem in melting, molten nickel will not wet thoria, and hence the thoria within the weld nugget will tend to agglomerate and float to the surface. With high welding rates, much of the thoria can be entrapped within the weld nugget, but in general, the strength of the weld nugget is reduced. Electron beam and ultrasonic welding may prove suitable for joining the material with a minimum sacrifice in properties. A graphic comparison of

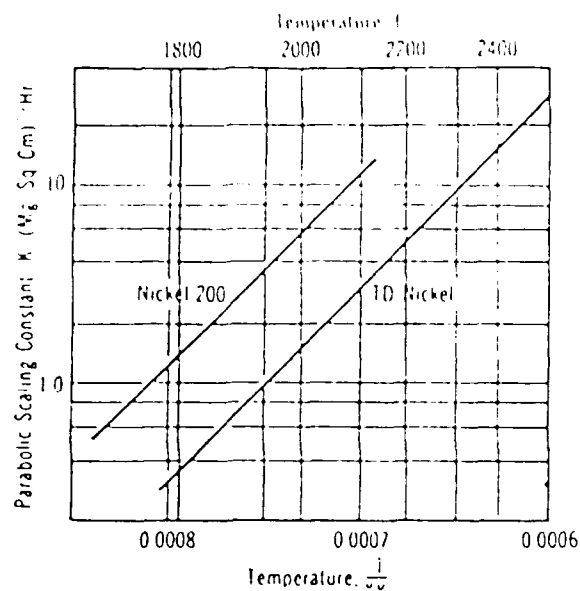


Fig. 5 — Parabolic scaling rates of TD nickel and nickel-200 are compared from 1800 to 2400 F. Test was run in static air.

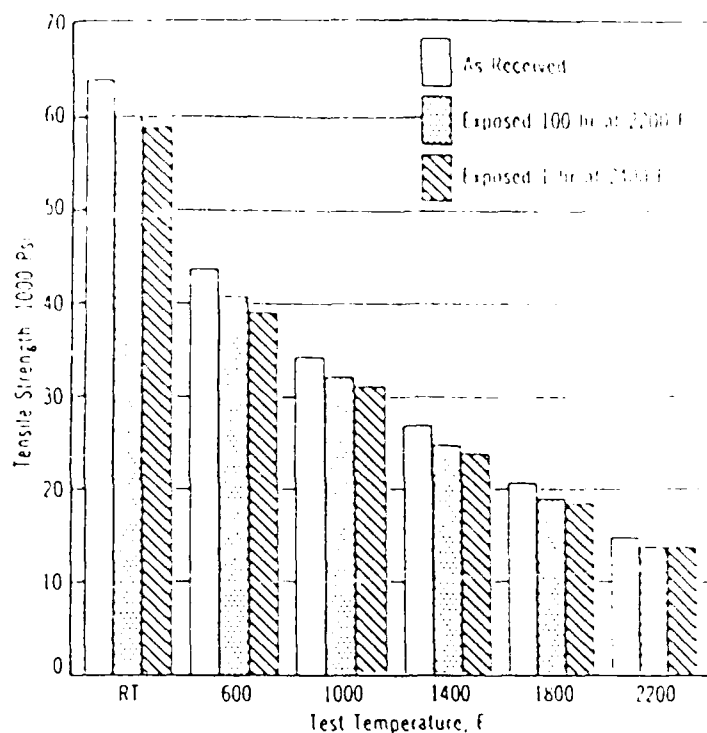


Fig. 6 — The effect of high-temperature exposure on the tensile strength of TD nickel is relatively minor.

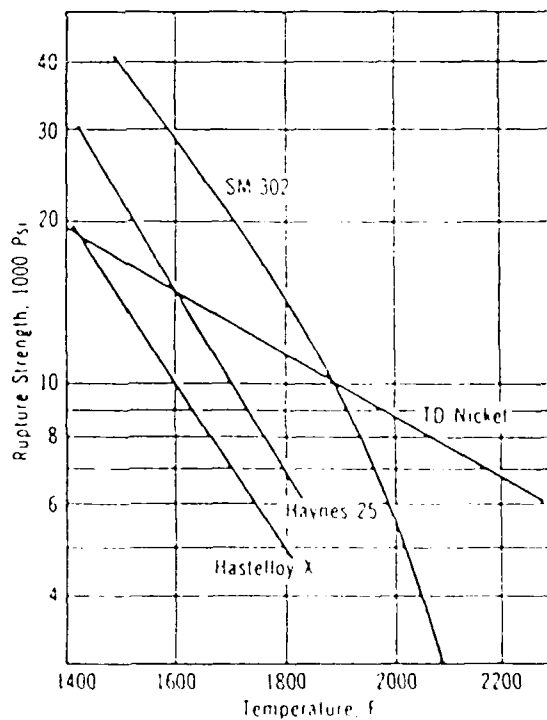


Fig. 7 — Curves compare 100-hr stress-rupture strength of TD nickel, Hastelloy X (47 Ni, 22 Cr, 20 Fe, 9 Mo), Haynes 25 (51 Co, 20 Cr, 15 W, 10 Ni) and SM-302 (57 Co, 22 Cr, 10 W, 9 Ta)

ESHIBIT 21

TD nickel with other high-temperature materials is shown in Fig. 7 (Exhibit 21). Because of its insensitivity to overheating, excellent creep properties and reliability at high temperatures, TD nickel will be a strong contender for applications such as jet engine nozzle vanes, high-temperature heat exchangers and supports (where temperature cycling and inadequate control is involved).

Bibliography

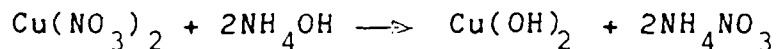
1. "TD Nickel, Dispersion Strengthened Nickel," DuPont Metal Products, Product Information, Pigments Department, E. I. duPont de Nemours & Co., 1965 (Rev).
2. "TD Nickel, A Dispersion Strengthened Metal," Fansteel, Inc., Metals Division, Bulletin TD-007-1.
3. F. J. Anders, Jr., G. B. Alexander, W. S. Wartel, Metal Progress, Dec. 1982, p. 88.
4. C. J. Bradford, Steel, oct. 31, 1982.
5. C. R. Manning, Jr., D. M. Royster, D. N. Braski, "An Investigation of a New Nickel Alloy Strengthened by Dispersed Thoria", NASA, Technical Note D-1944, Washington, July 1963, 38 pages.
6. J. E. White and R. D. Cainham, Trans AIME, 230; 1298-1306, October 1964.
7. S. G. Berkley, Pratt and Whitney Aircraft, "An Advanced Jet Engine Sheet Alloy - Coated TD Nickel", ASM National Metals Congress, Chicago, Ill. 1967.

5.3 ODS Aluminum

Alumina stability: Based on the work at DuPont rate of growth of alumina in copper at 800 C for 24 hours (see 5.1), it is not expected that alumina will coarsen during use at 500 - 600 C in a cast ODS aluminum. Any growth that will occur, probably already has occurred during casting. This appears to be minimal.

IPS: Figure 22 shows the relationship between IPS, oxide particle diameter and oxide volume loading and figure 23 shows how the strength of TD Nickel alloys varie with IPS. In the case of ODS aluminum, the particle size of the dispersoid is expected to be 0.02-0.03 micron and hence the effect of hardening in ODS Aluminum will be achievable at a much lower volume loading than was used in TD Nickel. (Smaller particles mean fewer particles at the same IPS.)

The Process: Apparatus used to prepare the copper-alumina is shown in Figure 2. Solutions containing the colloidal oxide particles, the dissolved reducible metal salt (copper nitrate) and base for precipitating the reducible metal salt as a hydroxide (ammonium hydroxide) are added at a controlled rate to a vigorously stirred vessel. When the metal salt solution and the base come together, the following reaction occurs:



which results in the precipitation of the copper hydroxide $[\text{Cu}(\text{OH})_2]$. The precipitates form around the colloidal oxide particles, preventing the oxide particles from coming in contact with each other as the precipitated copper hydroxide is filtered,

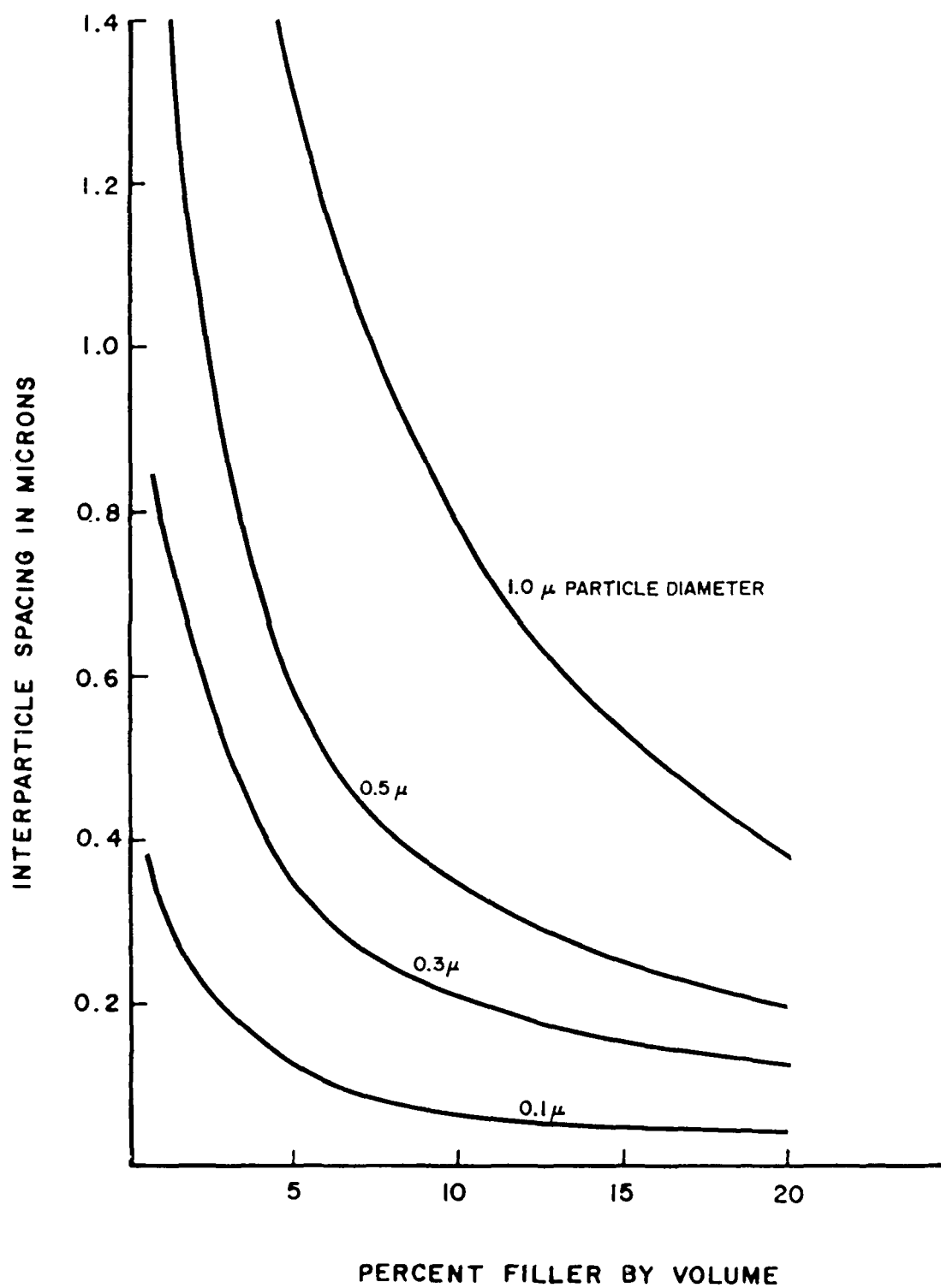


FIGURE 22

T D NICKEL
SHOWS THE EFFECT OF IPS ON STRENGTH

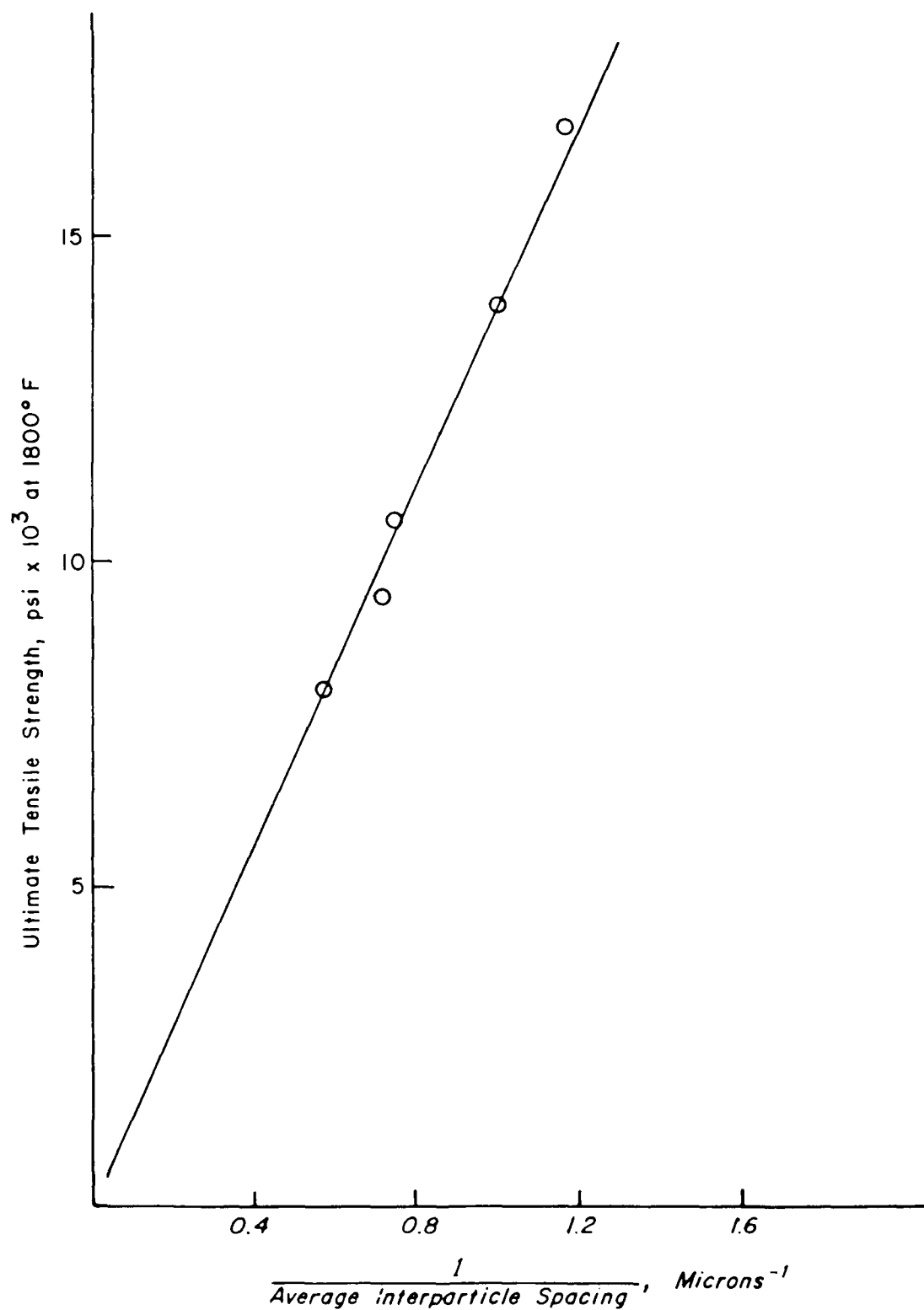


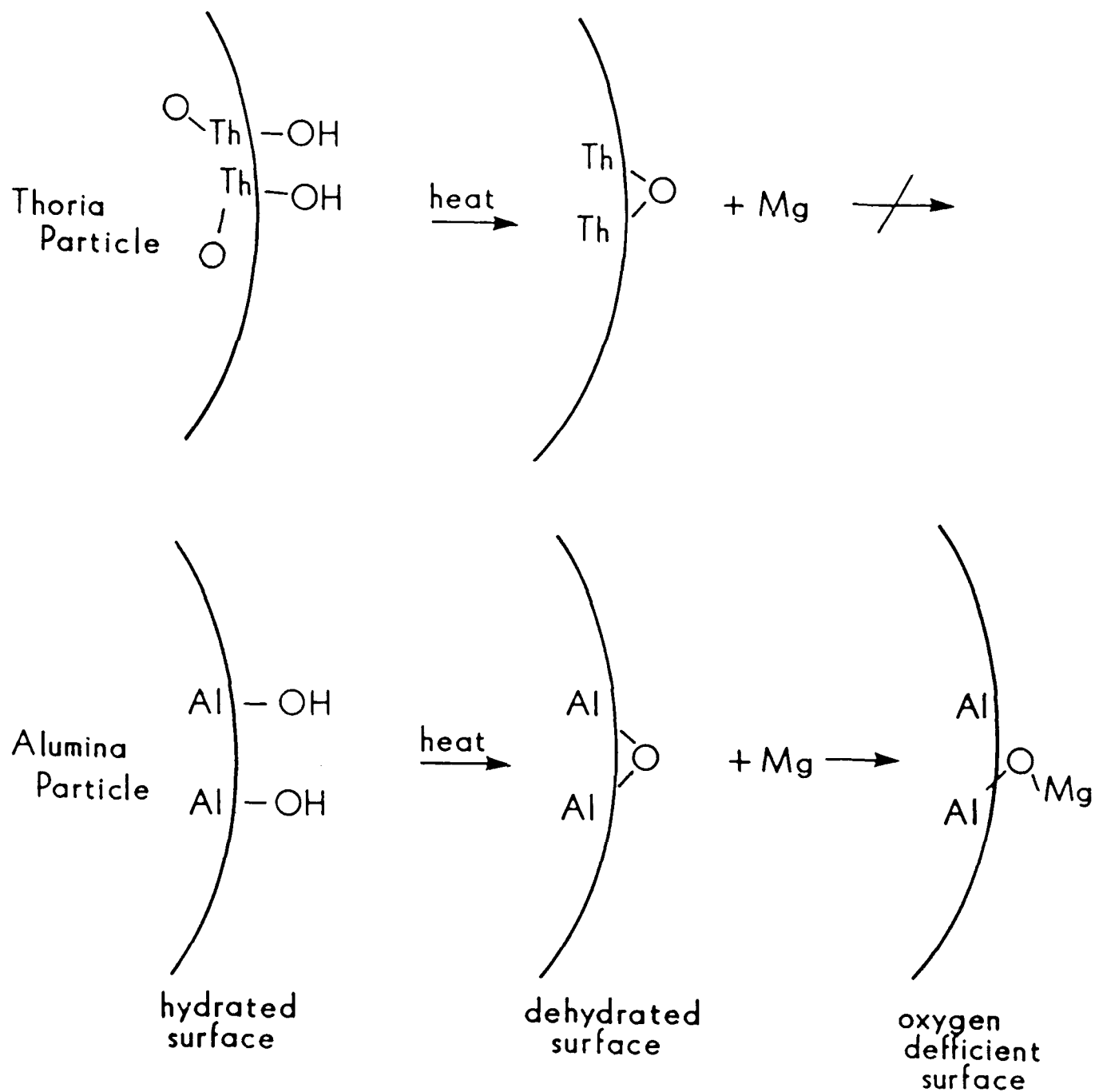
FIGURE 23

washed and dried. The problems of gelation or coagulation of the alumina (See 5.1.2) are thus avoided.

The copper hydroxide containing the dispersed oxide is reduced to metallic copper in hydrogen, pressed into a pellet and stored in an inert atmosphere to prevent any reaction with atmospheric oxygen. When the pellet is added to molten aluminum, the copper dissolves and the oxide particles disperse into the molten aluminum.

Wetting: Ceramic oxide particles are normally coated with an oxide or hydroxide surface, which is not normally wettable by molten metals. Based on Phase I results, a reaction on the oxide surface must occur before the oxide is wet by the molten metal.

One measure of an oxide's stability is its heat of formation. Table 2 lists the heats of formation of a number of metallic oxides. Thorium oxide (ThO_2) has a higher heat of formation than aluminum oxide or magnesium oxide (MgO). If thorium oxide is dispersed in a molten aluminum alloy containing magnesium, no reaction occurs between the surface of the thoria particles and the magnesium as shown in Figure 24. Aluminum oxide, however, has a lower heat of formation than magnesium oxide; therefore, when alumina particles are dispersed in molten aluminum containing magnesium, a reaction between the alumina surface and the magnesium metal is expected. It is theorized that this reaction is responsible for the wetting of alumina particles in an aluminum, magnesium alloy which was observed in Phase I. Figure 24 illustrates this reaction. Figure 25 is the flow sheet for the ODS aluminum process.

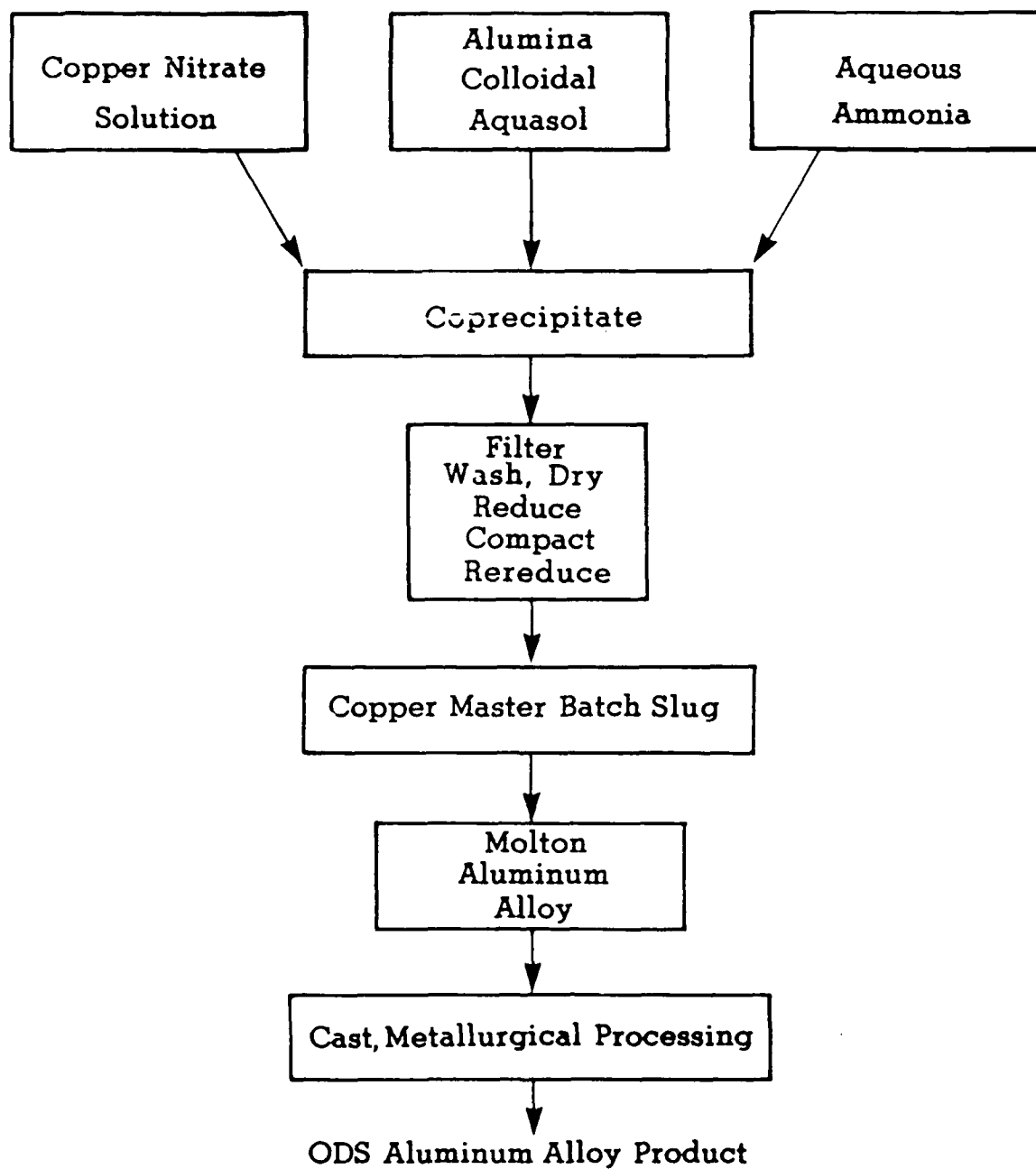


Reactions of Colloidal Oxides with Metals

FIGURE 24

ODS
New Aluminum Alloy

Process



Joinability: ODS aluminum should be joinable by all techniques currently used in aluminum fabrication. Because the oxide particles are stable in molten aluminum, welded joints should be as strong as the base aluminum alloy.

Table 2

Free Energies of Formation at 1800° F.

Y_2O_3	125
CaO	122
La_2O_3	121
BeO	120
ThO_2	119
MgO	112
UO_2	105
HfO_2	105
CeO_2	105
Al_2O_3	104
ZrO_2	100
BaO	97
$ZrSiO_4$	95
TiO	95
TiO_2	85
SiO_2	78
Ta_2O_5	75
V_2O_5	74
NbO_2	70
Cr_2O_3	62

6. Commercial Potential

6.1 Civilian Uses

Aluminum alloys are commercially used to a large degree due to relatively low cost, ease of working, availability, corrosion resistance and favorable strength to weight ratio. The 2000 series of aluminum alloys are used in aircraft structures, auto body panels, frames, and screw machine parts. It is probable that if an aluminum alloy was available which had improved high temperature properties, additional uses would become apparent, particularly if the treatment to achieve optimum mechanical properties could be simplified or eliminated.

Cast aluminum alloy pistons are used almost exclusively in gasoline powered engines. Current automotive demands are at the limit of commercially available cast aluminum alloys. Engine operating temperatures require the pistons to operate at 300° C pressures may exceed 2,000 psi. Current automotive engine designs demand between 75 and 100 hp per liter of engine displacement. Currently available aluminum alloys, when subjected to these operating conditions over their 10,000,000 cycle life, fail in a number of ways. Over the life of the piston, the hardness of the metal continues to decrease. Cracks may form in the top of the piston. Ring grooves expand as the yield stress of the metal is exceeded by the high temperature pounding of the steel rings. If the piston material is changed to non aluminum, higher strength, higher density alloy, a significant penalty in available energy is incurred.

TRA believes that our ODS aluminum alloy will provide improved high temperature properties over those alloys currently available, and that use temperatures may reach 500-550° C, allowing the development of automobile engines with better longevity or power to weight ratios over those currently available.

6.2 Military Uses

ODS aluminum alloys may provide significant benefit in military applications. Aircraft structures and skins are exposed to high temperatures in supersonic flight. ODS aluminum alloys which have improved temperature resistance may allow higher design velocities in aircraft that currently utilize aluminum components in high temperature applications. Additionally, it may be possible to replace higher cost titanium based alloys with ODS aluminum alloys in some applications where the service temperature exceeds the capabilities of current aluminum alloys.

Another possible application of ODS aluminum is high strength components which would be field repairable and would retain their high strength without subsequent heat treatment.

Current high strength aluminum alloys are heat treated to achieve their high strength properties. When such alloys are welded without subsequent heat treatment, the strength in the weld area is decreased. ODS alloys may have strength characteristics which do not rely on the same mechanism as heat treatable alloys, allowing structures to be field welded without a large compromise in the strength of the final part.

6.3 Commitment for Follow-On Funding

TRA is excited about the potential for ODS Aluminum, commercially. Their commitment taken from the Phase II proposal to continue the development into Phase III is summarized below. TRA has successfully raised over \$1,000,000 for other developments, and based on this track record, is confident of their ability to perform as indicated below.

TRA will provide \$2,000,000, 10% of which will be available on or before July 1, 1986, provided Phase II indicates that ODS Aluminum is a commercially feasible product. The \$2,000,000 will be used to design, construct and operate a pilot plant for the production of up to 5000 lbs. of ODS Aluminum/day.

The ODS Aluminum so produced will be used for a market evaluation of the product.

Funding Schedule

7/1/86	\$50,000	Cost estimate
7/1/86	\$50,000	Market survey
8/1/86	\$70,000	Design
10/1/86	\$800,000	Construction
1/1/87	\$500,000	Start up
1/1/87	\$200,000	Contingency
4/1/87	\$150,000	Operation
7/1/87	\$180,000	Operation

This commitment was approved by the Board of Directors March 2, 1984.

7. Proposed Publication

M. R. Plichta, J. K. Weeks and G. B. Alexander, "ODS Aluminum - An Electromicrographic Study," journal to be selected.

Additional data from Phase II will be required before this paper can be published.

Todate, there are no publications

8. Personnel

Guy B. Alexander, Principal Investigator

Joseph K. Weeks, Project Manager

Bruce Scarbrough, Technician

Paul Bennett, Technician

In-Ok Shim, Metallurgist

Professor J. G. Byrne, Consultant

Professor M. R. Plichta, Microscopist-metallurgist

Wayne O. Ursenbach, Consultant

Charles Baker, Equipment Design

Resumes available on request.

No degrees awarded from these studies

9. Interactions.

None.

10. New Discoveries

Based on an opinion of Alvin D. Shulman (1), who has conducted a patent search on the ODS aluminum process, the process and

product appear to be patentable. TRA intends to to file a patent on the subject.

(1) Alvin D. Shulman of Marshall, O'Toole, Gerstein, Murrah and Bicknell, a legal partnership, 20 South Clark St., Chicago, Ill., 60603 to G. B. Alexander 3/19/84, "Method of Producing Copper-Aluminum alloy containing Alumina Particles."

REPORT ON

"Aluminum Oxide Dispersion in Al-4Cu-3Mg"

Prepared by

Dr. Mark R. Plichta

Assistant Professor

Department of Materials Science and Engineering

University of Utah

Salt Lake City, Utah 84112

for

Technical Research Associates, Inc.

Suite 222

410 Chipeta Way

Salt Lake City, Utah 84108

March 28, 1984

Introduction:

This report summarizes the results obtained during the investigation of the microstructure in an Al-4Cu-3Mg alloy doped with Al_2O_3 particles. Thin foils of the materials were prepared in a dual jet electropolisher. The electrolyte employed was 750 ml methanol, 225 ml glycerol and 25 ml perchloric acid. Polishing was performed at 25°C using a voltage of 26 V to 30 V. Perforated 3 mm discs were cleaned immediately in ethanol. The specimens were examined with a JEM-200 CX electron microscope operating at 200 kV. Qualitative chemical analyses of the various microconstituents were obtained through Energy Dispersive Spectroscopy (EDS) using a KEVEX detector and analyzer.

Description of Microstructure

The microstructure of the alloys, as observed in TEM, consisted of three distinctly different particles in an aluminum matrix. The first type of particle was found exclusively at grain boundaries and had a very smooth, spherical morphology. When analyzed with EDS the composition of these particles was found to be primarily Si and O (Fig. 1). This strongly suggests that these particles are silica, and are likely present as an impurity oxide.

The second type of particle was comparable in size to the silica particles (i.e., 1 to 5 μm) and was also located primarily at grain boundaries. Chemical analysis of these particles found them to be primarily Al with a large amount of Cu and O, and a small amount of Mg (fig. 2). Figure 3a shows one of these particles, and it is highly probable that these particles are θ precipitates. Upon close examination of this particle, it can be seen that it contains a uniform dispersion of very small, yet distinct, particles. When a dark field image is obtained using a portion of the diffraction ring

formed by the Al_2O_3 particles, these small particles in the " θ " precipitates light up as shown in Figure 3b. This strongly suggests that these particles are Al_2O_3 and also explains the high oxygen content in these θ precipitates.

These small Al_2O_3 particles which are on the order of 300 \AA in diameter represent the third type of particle observed in this material. They were not only observed in the " θ " precipitates but were also found to be uniformly dispersed in the aluminum matrix. Figure 4a is a bright field image of the aluminum matrix showing the dispersion of the Al_2O_3 particles while figure 4b is again a dark field image of the same area formed by using a portion of an Al_2O_3 diffraction ring. Figure 5 is the EDS spectrum for the matrix which shows the presence of oxygen and supports the suggestion that these intragranular particles are indeed Al_2O_3 .

Explanation for Observed Microstructure and Possible Effects on Mechanical Properties

Based on the author's observations of the microstructure in this material the following explanation seems the most probable for its microstructural evolution:

1). The SiO_2 particles were likely introduced in the melt at some point, and are there as an impurity particle. They can be eliminated with appropriate alloying procedures.

2). It is this author's opinion that the so called θ precipitates are actually a remnant of incomplete dissolution of the Al_2O_3 containing Cu slugs which were introduced into the aluminum melt. This opinion is based on the fact that the precipitates still contain a high concentration of randomly dispersed Al_2O_3 particles. This random dispersion would be extremely unlikely if the θ precipitates had formed during a solid state transformation.

3) The Al_2O_3 particles present in the aluminum matrix are there as a result of the partial dissolution of the Cu slugs.

It appears then that this material has a strong potential for oxide dispersion strengthening. It is the authors opinion that, even at the observed oxide particle densities in the aluminum matrix, considerable strengthening can be achieved. In addition, complete dissolution of the Cu slugs will make this effect even more pronounced.

This material would have two distinct advantages over conventional precipitation hardened aluminum alloys. First, the particles which strengthen this material, i.e. Al_2O_3 , will be stable and remain present at higher temperatures than the θ' or θ'' precipitates that typically strengthen aluminum alloys. This would then increase the possible operating temperature of aluminum by approximately $200^{\circ}C$. Second, the size stability of these particles should be good even at elevated temperatures since any particle coarsening would require oxygen diffusion through the aluminum which should be relatively slow at temperatures of interest.

16-Mar-1983 13:26:26

-WARNING-

SMOOTH PARTICLE

Preset= 100 secs

Vert= 5000 counts Disp= 1

Elapsed= 100 secs

Si

AL-4CU-6MG WITH 10 PCT

AL2O3 FILLER

SMOOTH PARTICLE

Mg

Cl Sn

Cu

0.360

Range=

10.230 keV

10.230

Integral 9 =

151142

17-Mar-1983 12:19:06

CHI Sensor

PRECIPITATE

Vert= 5000 counts Disp= 1

Preset=

100 sec

Elapsed=

100 sec

Al

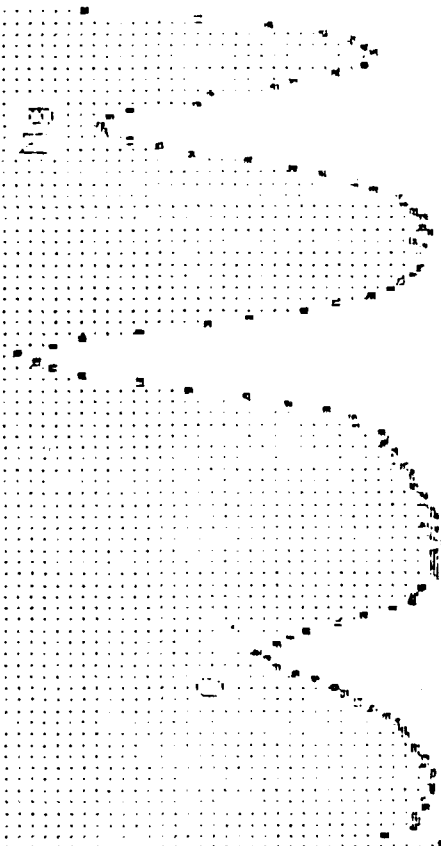
AL-4CU-3MG WITH 10 PCT

AL2O3 FILLER

PRECIPITATE COMPOSITION

Cu

Mg



0.240 Range= 10.230 keV

5.760

0

51300



Figure 3. Al-4Cu-3Mg with 10% Al₂O₃ filler. a) Bright field of a "θ" precipitate, and b) dark field image using a portion of an Al₂O₃ diffraction ring. 4000X.



Figure 4. Al-4Cu-3Mg with 10% Al_2O_3 filler. a) Bright field of an aluminum matrix grain, and b) dark field image using a portion of an Al_2O_3 diffraction ring. 27000X.

17-Mar-1983 12:08:12

-WARNING-

MATRIX

Vert= 2000 counts Disp= 1

Preset= 100 sec

Elapsed= 100 sec

INSTRUMENT AREA

Al

AL-4CU-3MG WITH 10 PCT

AL2O3 FILLER

MATRIX COMPOSITION

Mg

0.340 Range= 10.230 keV

Integral 0 = 16384

THE
UNIVERSITY
OF UTAH

DEPARTMENT OF
MATERIALS SCIENCE
AND ENGINEERING

SALT LAKE CITY UTAH 84112
801 581 6863

March 29, 1984

Dr. Guy Alexander
Technical Research Associates, Inc.
Suite 222
410 Chipeta Way
Salt Lake City, Utah 84108

Dear Dr. Alexander:

From reviewing the results of Dr. Mark R. Plichta, in particular, Fig. 4 of his report of March 28, 1984, to TRA, I find that the closest spacing of fine Al_2O_3 particles in an Al matrix is from 0.5 to 1.0 μm at 27,000 magnifications, or from 3700 \AA to 1850 \AA approximately. This kind of separation distance is ideal for effective dispersion hardening. In fact, the lower figure is about in the range where rigid dislocation-particle interactions, of the type found at peak hardness in G.P. zone containing Al-Cu base alloys may become possible. The latter type interaction could give yield strength values to those provided by oxide dispersion hardening. At the very least, however, the objective of producing a stable oxide dispersion hardened Al base alloy appears to have been successfully achieved.

Sincerely yours,


J. G. Byrne
Professor

In